

การสังเคราะห์และฤทธิ์ต้านแบคทีเรียของวัสดุเซลลูโลสที่มีหมู่แอมิโน

นางสาวมนรวิศ รวยชนพานิช



บทคัดย่อและแฟ้มข้อมูลฉบับเต็มของวิทยานิพนธ์ตั้งแต่ปีการศึกษา 2554 ที่ให้บริการในคลังปัญญาจุฬาฯ (CUIR)  
เป็นแฟ้มข้อมูลของนิสิตเจ้าของวิทยานิพนธ์ ที่ส่งผ่านทางบัณฑิตวิทยาลัย

The abstract and full text of theses from the academic year 2011 in Chulalongkorn University Intellectual Repository (CUIR)  
are the thesis authors' files submitted through the University Graduate School.

วิทยานิพนธ์นี้เป็นส่วนหนึ่งของการศึกษาตามหลักสูตรปริญญาวิทยาศาสตรมหาบัณฑิต

สาขาวิชาเคมี ภาควิชาเคมี

คณะวิทยาศาสตร์ จุฬาลงกรณ์มหาวิทยาลัย

ปีการศึกษา 2558

ลิขสิทธิ์ของจุฬาลงกรณ์มหาวิทยาลัย

SYNTHESIS AND ANTIBACTERIAL ACTIVITIES OF AMINO-CONTAINING  
CELLULOSIC MATERIALS

Miss Monrawat Rauytanapanit



A Thesis Submitted in Partial Fulfillment of the Requirements  
for the Degree of Master of Science Program in Chemistry

Department of Chemistry

Faculty of Science

Chulalongkorn University

Academic Year 2015

Copyright of Chulalongkorn University

Thesis Title	SYNTHESIS AND ANTIBACTERIAL ACTIVITIES OF AMINO-CONTAINING CELLULOSIC MATERIALS
By	Miss Monrawat Rauytanapanit
Field of Study	Chemistry
Thesis Advisor	Thanit Praneenararat, Ph.D.

---

Accepted by the Faculty of Science, Chulalongkorn University in Partial  
Fulfillment of the Requirements for the Master's Degree

.....Dean of the Faculty of Science  
(Associate Professor Polkit Sangvanich, Ph.D.)

THESIS COMMITTEE

.....Chairman  
(Associate Professor Vudhichai Parasuk, Ph.D.)

.....Thesis Advisor  
(Thanit Praneenararat, Ph.D.)

.....Examiner  
(Assistant Professor Sumrit Wacharasindhu, Ph.D.)

.....External Examiner  
(Duangrudee Tanramluk, Ph.D.)

มนรวิศ รวยธนพานิช : การสังเคราะห์และฤทธิ์ต้านแบคทีเรียของวัสดุเซลลูโลสที่มีหมู่แอมิโน (SYNTHESIS AND ANTIBACTERIAL ACTIVITIES OF AMINO-CONTAINING CELLULOSIC MATERIALS) อ.ที่ปรึกษาวิทยานิพนธ์หลัก: อ. ดร.ธนิชช์ ปราณีนรารัตน์, 49 หน้า.

การเกิดไบโอฟิล์มและการเกาะติดของแบคทีเรียบนพื้นผิวเป็นปัญหาสำคัญในทางสาธารณสุข และอุตสาหกรรมต่างๆ เพื่อแก้ปัญหาเหล่านี้จึงได้มีการพัฒนาวัสดุต้านเชื้อแบคทีเรียที่ออกฤทธิ์เมื่อมีการสัมผัสของแบคทีเรียบนพื้นผิว โดยงานวิจัยนี้ศึกษาการตรึงสารประกอบแอมิโนกลุ่มต่างๆ ได้แก่ 3-aminopropyltrimethoxysilane (APS), polyethyleneimine (PEI), 1,4-diazabicyclo[2.2.2]octane (DABCO) และ 4,7,10-trioxa-1,13-tridecanediamine (DA) ลงบนพื้นผิวของผ้าฝ้ายด้วยปฏิกิริยาเคมีต่างๆ ทดสอบสมบัติทางกายภาพของพื้นผิวด้วยเทคนิค ATR-FTIR, XPS และ SEM ตรวจสอบปริมาณหมู่แอมิโนแบบปฐมภูมิ และจุลทรรศน์บนพื้นผิวสังเคราะห์โดยใช้ CI acid orange 7 และ fluorescein sodium salt ตามลำดับ ทดสอบฤทธิ์ต้านแบคทีเรียของพื้นผิวสังเคราะห์ด้วยวิธีการนับโคโลนี (JIS L 1902) กับแบคทีเรียแกรมบวก (*Staphylococcus aureus* (ATCC 6538P) และแบคทีเรียแกรมลบ (*Escherichia coli* (ATCC 8739) and *Pseudomonas aeruginosa* (ATCC 9027)) ผลการศึกษาพบว่า DABCO-C16 ซึ่งเป็นพื้นผิวที่มีประจุบวกถาวร และ Phys.PEI ซึ่งพื้นผิวสามารถเกิดประจุบวกได้จากการรับโปรตอน สามารถยับยั้งการเติบโตของแบคทีเรียทั้งแกรมบวกและแกรมลบ โดยไม่พบโคโลนีใดๆบนพื้นผิว นอกจากนี้ แม้ว่าพื้นผิว APS และ DA จะไม่สามารถยับยั้งการเติบโตของแบคทีเรียได้ทั้งหมด แต่ถือว่ามีฤทธิ์การต้านเชื้อแบคทีเรียที่แรงเช่นกัน โดยลดจำนวนโคโลนีของแบคทีเรียได้ถึง 5 ลอการิทึม นอกจากนี้มีการทดสอบความเป็นพิษของพื้นผิวต่อเซลล์ไฟโบรบลาสต์ของหนู (L-929) ผลการทดสอบแสดงถึงความเข้ากันได้ทางชีวภาพของพื้นผิว DABCO, DA และอนุพันธ์ของ DA กับเซลล์ของสัตว์เลี้ยงลูกด้วยนม

ภาควิชา เคมี

ลายมือชื่อนิสิต .....

สาขาวิชา เคมี

ลายมือชื่อ อ.ที่ปรึกษาหลัก .....

ปีการศึกษา 2558

# # 5672054723 : MAJOR CHEMISTRY

KEYWORDS: ANTIBACTERIAL CELLULOSE / COTTON FABRIC

MONRAWAT RAUYTANAPANIT: SYNTHESIS AND ANTIBACTERIAL ACTIVITIES OF AMINO-CONTAINING CELLULOSIC MATERIALS. ADVISOR: THANIT PRANEENARARAT, Ph.D., 49 pp.

Biofilm formation and bacteria adhesion on surfaces are major problems for both public health and several industries. To solve these problems, considerable attention has been directed toward developing contacted-based bactericidal surfaces. In this research, series of amino-containing molecules including 3-aminopropyltrimethoxysilane (APS), polyethyleneimine (PEI), 1,4-diazabicyclo[2.2.2]octane (DABCO), and 4,7,10-trioxa-1,13-tridecanediamine (DA) were immobilized on cotton surfaces via various chemical reactions. The physical properties of these surfaces were determined using Attenuated Total Reflection Fourier Transform Infrared Spectroscopy (ATR-FTIR), X-ray Photoelectron Spectroscopy (XPS), and Scanning Electron Microscopy (SEM). Primary and quaternary amine loading were quantified using Cl acid orange 7 and fluorescein sodium salt, respectively. Antibacterial activities of all surfaces were evaluated using colony counting method (JIS L 1902) in both Gram-positive (*Staphylococcus aureus* (ATCC 6538P) and Gram-negative bacteria (*Escherichia coli* (ATCC 8739) and *Pseudomonas aeruginosa* (ATCC 9027)). DABCO-C16 with permanent positive charges and Phys.PEI with the abilities to be protonated showed broad-spectrum antibacterial activities with complete killing. Although APS and DA did not show complete killing, they were still considered highly active with around 5 log CFU reduction. Moreover, cytotoxicity assays of modified cottons toward L-929 mouse connective tissue fibroblast were conducted. The results confirmed that DABCO and DA and its derivative were biocompatible with mammalian cells.

Department: Chemistry

Student's Signature .....

Field of Study: Chemistry

Advisor's Signature .....

Academic Year: 2015

## ACKNOWLEDGEMENTS

I would first like to thank my thesis advisor Dr. Thanit Praneenararat of the Department of Chemistry, Faculty of Science, Chulalongkorn University for his support and motivation. His guidance and encouragement always make me feel warm since the beginning of my research to present.

Besides my advisor, I would like to thank Assistant Professor Dr. Rungaroon Waditee Sirisattha of the Department of Microbiology, Faculty of Science, Chulalongkorn University and Assistant Professor Dr. Hajime Takahashi of the Department of Food Science and Technology, Tokyo University of Marine Science and Technology, Japan for offering me the precious opportunities in their groups and leading me working on diverse exciting projects.

My sincere thanks also go to my thesis committee: Associate Professor Dr. Vudhichai Parasuk, Assistant Professor Dr. Sumrit Wacharasindhu and Dr. Duangrudee Tanramluk. I am gratefully indebted to them for their very valuable questions and comments on this thesis.

I would also like to thank the development and promotion of science and technology talents project (DPST) and Ratchadaphiseksomphot Endowment Fund for the financial supports and the experts who were involved in the validation survey for this research project.

Finally, I must express my bottomless thanks to my family, my friends and all members in TP and RWS labs for providing me with continuous support throughout many years of the study. This accomplishment would not have been possible without them. Thank you.

## CONTENTS

	Page
THAI ABSTRACT .....	iv
ENGLISH ABSTRACT .....	v
ACKNOWLEDGEMENTS .....	vi
CONTENTS .....	vii
LIST OF FIGURES .....	x
LIST OF SCHEMES .....	xii
LIST OF TABLE .....	xiii
LIST OF ABBREVIATIONS .....	xiv
CHAPTER I INTRODUCTION .....	1
1.1 Bacterial infection.....	1
1.2 Bacterial membrane components.....	1
1.3 Mechanism of antibacterial surfaces.....	2
1.4 Antibacterial cellulose.....	4
CHAPTER II EXPERIMENT.....	12
2.1 Materials .....	12
2.2 Synthesis of amino-containing surfaces .....	12
2.2.1 Synthesis of APS-modified surface (APS).....	12
2.2.2 Synthesis of IO <sub>4</sub> /PEI-modified surfaces (IO.PEI).....	13
2.2.3 Synthesis of OTs/PEI modified surface (TS.PEI).....	13
2.2.4 Fabrication of physically-adsorbed PEI surface (Phys.PEI).....	14
2.2.5 Synthesis of DABCO modified surface (DABCO).....	14
2.2.6 Synthesis of DABCO-C16 modified surface (DABCO-C16).....	15

	Page
2.2.7 Synthesis of DA modified surface (DA).....	16
2.3 Characterization .....	18
2.3.1 Primary amine loading quantification by Cl acid orange 7.....	18
2.3.2 Quaternary amine loading quantification by fluorescein sodium salt	18
2.3.3 Attenuated Total Reflection Fourier Transform Infrared Spectroscopy (ATR-FTIR).....	19
2.3.4 X-ray Photoelectron Spectroscopy (XPS).....	19
2.3.5 Scanning Electron Microscopy (SEM).....	19
2.4 Antibacterial activity assays.....	19
2.5 Inhibitory activities against foodborne pathogens .....	20
2.6 Cytotoxicity assay .....	21
CHAPTER III RESULTS AND DISCUSSION .....	22
3.1 Synthesis of amino-containing surfaces .....	22
3.1.1 Synthesis of APS-modified surface (APS).....	23
3.1.2 Synthesis of IO4/PEI-modified surfaces (IO.PEI).....	23
3.1.3 Synthesis of OTs/PEI modified surface (TS.PEI).....	24
3.1.4 Fabrication of physically-adsorbed PEI surface (Phys.PEI) .....	24
3.1.5 Synthesis of DABCO modified surface (DABCO) .....	24
3.1.6 Synthesis of DABCO-C16 modified surface (DABCO-C16).....	25
3.1.7 Synthesis of DA modified surface (DA).....	25
3.2 Characterization .....	27
3.2.1 Primary amine loading quantification.....	27
3.2.2 Quaternary amine loading quantification.....	29



	Page
3.2.3 ATR-FTIR experiments .....	31
3.2.4 Elemental compositions by XPS analysis.....	32
3.2.5 Surface morphology by SEM analysis.....	34
3.3 Antibacterial activities.....	37
3.4 Inhibitory activities against foodborne pathogens .....	40
3.5 Cytotoxicity .....	42
CHAPTER IV CONCLUSIONS.....	43
REFERENCES .....	44
VITA.....	49



## LIST OF FIGURES

<b>Figure 1.1</b> The cell envelopes of Gram-positive (left) and Gram-negative (right) bacteria .....	2
<b>Figure 1.2</b> Antibacterial mechanism of released-based (left) and contact-based (right) bactericidal surfaces .....	3
<b>Figure 1.3</b> Chemical structure of cellulose.....	4
<b>Figure 1.4</b> Synthetic scheme of DABCO-R surfaces (R vary from C8 to C18).....	5
<b>Figure 1.5</b> Synthetic scheme of DABCO derivative modified methyl $\alpha$ -D-glucopyranoside.....	6
<b>Figure 1.6</b> Synthetic scheme of PEI derivatives modified cotton and wool.....	7
<b>Figure 1.7</b> Molecular structure of <i>N,N,N</i> -ANPAH,dodecyl,methyl-PEI .....	8
<b>Figure 1.8</b> Synthetic scheme of GMA modified nanofibrillar cellulose.....	8
<b>Figure 1.9</b> Synthetic scheme of APS modified bacterial cellulose .....	9
<b>Figure 1.10</b> Mechanism of acetone induced polymerization of APS .....	10
<b>Figure 1.11</b> Synthetic scheme of diamino spacer chains modified cotton.....	10
<b>Figure 3.1</b> Molecular structure of CI acid orange 7.....	28
<b>Figure 3.2</b> Calibration curve of CI acid orange in 25% aq. pyridine solution.....	28
<b>Figure 3.3</b> Molecular structure of fluorescein sodium salt.....	29
<b>Figure 3.4</b> Calibration curve of fluorescein sodium salt in 0.25% aq. CTAB.....	30
<b>Figure 3.5</b> ATR-FTIR spectra of unmodified and modified cottons. ....	31
<b>Figure 3.6</b> XPS survey scan spectra of unmodified and modified cottons .....	32
<b>Figure 3.7</b> Curve fitting results of C1s scan spectra.....	33
<b>Figure 3.8</b> Curve fitting results of N1s scan spectra.....	34
<b>Figure 3.9</b> SEM images of unmodified and modified cotton with x500 magnification.....	35

<b>Figure 3.10</b> SEM images of unmodified and modified cotton with x5000 magnification.....	36
<b>Figure 3.11</b> Log CFU of <b>A)</b> <i>Staphylococcus aureus</i> <b>B)</b> <i>Escherichia coli</i> <b>C)</b> <i>Pseudomonas aeruginosa</i> after 18-h incubation on various surfaces .....	40
<b>Figure 3.12</b> Log CFU of <b>A)</b> Gram-positive and <b>B)</b> Gram-negative foodborne pathogens after 18-h incubation on various surfaces .....	41
<b>Figure 3.13</b> Cell viability on modified surfaces using L-929 cell line .....	42



## LIST OF SCHEMES

Scheme 2.1 Synthesis of APS-modified surface (APS).....	13
Scheme 2.2 Synthesis of IO <sub>4</sub> /PEI-modified surfaces (IO.PEI).....	13
Scheme 2.3 Synthesis of OTs/PEI modified surface (TS.PEI).....	14
Scheme 2.4 Synthesis of DABCO modified surface (DABCO).....	15
Scheme 2.5 Synthesis of the precursor molecule for DABCO.C16 fabrication.....	15
Scheme 2.6 Synthesis of DABCO-C16 modified surface (DABCO-C16).....	15
Scheme 2.7 Synthesis of DA modified surface (DA).....	16
Scheme 2.8 Further modifications of surface DA with additional reagents.....	18
Scheme 3.1 Chemical grafting of amino-containing molecules onto cellulose surfaces.....	22
Scheme 3.2 Synthesis of APS-modified surface (APS).....	23
Scheme 3.3 Mechanism of acetone-induced polymerization.....	23
Scheme 3.4 Synthesis of IO <sub>4</sub> /PEI-modified surfaces (IO.PEI).....	24
Scheme 3.5 Synthesis of OTs/PEI modified surface (TS.PEI).....	24
Scheme 3.6 Synthesis of DABCO modified surface (DABCO).....	25
Scheme 3.7 Synthesis of the precursor molecule for DABCO.C16 fabrication.....	25
Scheme 3.8 Synthesis of DABCO-C16 modified surface (DABCO-C16).....	25
Scheme 3.9 Synthesis of DA modified surface (DA).....	26
Scheme 3.10 Further modifications of surface DA with additional reagents.....	27

**LIST OF TABLE**

<b>Table 2.1</b> Strains and culture conditions of bacteria.....	20
<b>Table 2.2</b> Strains and culture conditions of foodborne pathogens. ....	21
<b>Table 3.1</b> Primary amine loading on surfaces.....	29
<b>Table 3.2</b> Quaternary amine loading on surfaces.....	30
<b>Table 3.3</b> Atomic concentration (%) in survey scan spectra.....	32



## LIST OF ABBREVIATIONS

ADSCs	Adipose derived stem cells
AgNPs	Silver nanoparticles
AMPs	Antimicrobial peptides
APS	3-aminopropyltrimethoxysilane
ATCC	American Type Culture Collection
ATR-FTIR	Attenuated Total Reflection Fourier Transform Infrared Spectroscopy
BC	Bacterial cellulose
CIP	Collection of Institute Pasteur
CFU	Colony forming unit
CTAB	Cetyltrimethylammonium bromide
DA	4,7,10-trioxa-1,13-tridecanediamine
DABCO	1,4-Diazabicyclo[2.2.2]octane
DIC	<i>N,N'</i> -diisopropylcarbodiimide
DMF	<i>N,N</i> -dimethylformamide
EG	Ethylene glycol
FBS	Fetal Bovine Serum
GMA	Glycidyl trimethyl ammonium chloride
HOBT	Hydroxybenzotriazole
IAM	Institute of Molecular and Cellular Biosciences
JCM	Japan Collection of Microorganisms
JIS	Japanese Industrial Standard
MIC	Minimum inhibitory concentration
MRSA	Methicillin-resistant <i>Staphylococcus aureus</i>
MRSB	de Man, Rogosa and Sharpe broth
MTT	3-(4,5-dimethylthiazol-2-yl)-2,5-diphenyltetrazolium bromide
NB	Nutrient broth
NFC	Nanofibrillar cellulose
NMR	Nuclear Magnetic Resonance spectroscopy
NSS	Normal saline solution

PEG	Polyethylene glycol
PEI	Polyethyleneimine
PUU	Polyurethane urea
PVA	Polyvinyl alcohol
QACs	Quaternary ammonium compounds
RPMI	Roswell Park Memorial Institute medium
SEM	Scanning Electron Microscopy
TSB	Trypticase Soy broth
TsCl	<i>p</i> -toluenesulfonylchloride
XPS	X-ray Photoelectron Spectroscopy



## CHAPTER I

### INTRODUCTION

#### 1.1 Bacterial infection

Bacterial attachment and proliferation on surfaces pose serious problems in both public health and industries [1]. For biomedical applications, bacterial adherence and biofilm formation on medical implants and devices limit the lifetime of devices, cause inflammatory responses and become antibiotic resistance bacteria. For marine industries, microbial attachment on a ship's hull induces other marine species to attach and proliferate, leading to high cost of fuel consumption and maintenance. For food industries, bacterial contaminations can occur during the raw materials storage and food productions, resulting in food contamination and spoilage. Foodborne illness or food poisoning is a result of consuming contaminated food [2]. It can seriously affect anyone, especially pregnant women and children. To solve these problems, considerable attention have been directed toward developing antibacterial agents and materials that can prevent bacterial attachment and proliferation.

#### 1.2 Bacterial membrane components

Several antibiotics are designed to destroy or interrupt the cell wall formation. The rigid bacterial cell wall provides structural integrity to the cell and protects the cell from swelling and rupturing caused by osmotic tension between cell and its surrounding. It usually consists of peptidoglycan, polysaccharide network interlaced by polypeptides. The different formations of peptidoglycan layer can be used to identify two major types of bacteria by a staining process called a Gram stain. The cell envelopes of Gram-positive and Gram-negative bacteria are shown in **Figure 1.1**. In Gram-positive bacteria, the peptidoglycan (red) forms a thick network around the outer surface and stains a purple color of crystal violet. The intercalated lipoteichoic acid (yellow) carries negative charges on bacterial cell wall due to the presence of phosphate in its structure. The peptidoglycan layer is relatively less abundant in the Gram-negative envelope, and is sandwiched between an outer membrane and the cell membrane. It does not retain the purple-colored dye, but gets stained by the dye



safranin. The outer membrane in the Gram-negative envelope is composed of phospholipid (green), protein porins (yellow), lipoproteins (blue) and lipopolysaccharides (green) which impart a negative charge to bacterial surface.

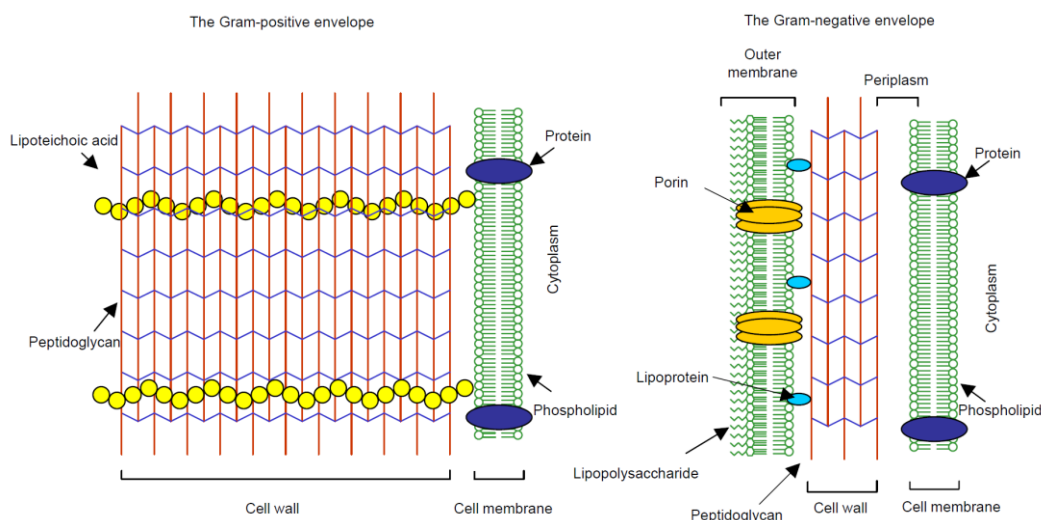


**Figure 1.1** The cell envelopes of Gram-positive (left) and Gram-negative (right) bacteria [3].

### 1.3 Mechanism of antibacterial surfaces

Various designed of antibacterial surfaces can be divided into two main categories [4] based on their operating strategies: bacteria-resistant surfaces and bactericidal surfaces.

Bacteria-resistant surfaces have a general purpose to reduce bacterial attachment on surfaces and thereby inhibit the earliest stages of biofilm formation by preventing non-specific adhesions of biologically related materials. These surfaces are usually modified with hydrophilic polymer to form the hydration layer as a physical barrier in aqueous environment. Oligomers based on different repeating units of ethylene glycol (EG) are the most commonly used. Chemical grafting of hydroxyl groups of polyethylene glycol (PEG) to isocyanate groups of polyurethane urea (PUU) surface was reported [5]. The modified surface forms a hydrophilic PEG layer that repels bacterial cells. This surface not only inhibited the accumulation of bacteria, but also showed a resistance for protein adsorption and platelet adhesion.

Bactericidal surfaces are surfaces with an ability to kill bacteria. These surfaces can be divided into released-based and contact-based bactericidal surfaces according to the killing mechanism as shown in **Figure 1.2**. For released-based bactericidal surfaces, biocidal agents are preloaded or coated on surfaces and slowly leached into surrounding to kill bacteria. Silver nanoparticles (AgNPs) are an example of common biocidal agents applied to antibacterial surfaces. AgNPs slowly release silver ions into the coating layer and subsequently the solution. AgNPs can attach to the bacterial membrane by electrostatic interaction, then leading to disruption of the membrane and consequently cell death [6]. However, these type of surfaces showed a temporary activity and may cause environmental problems. For human health, prolong contact with silver can cause irreversible pigmentation of the skin or eyes known as argyria and other serious effect on the kidney [7].

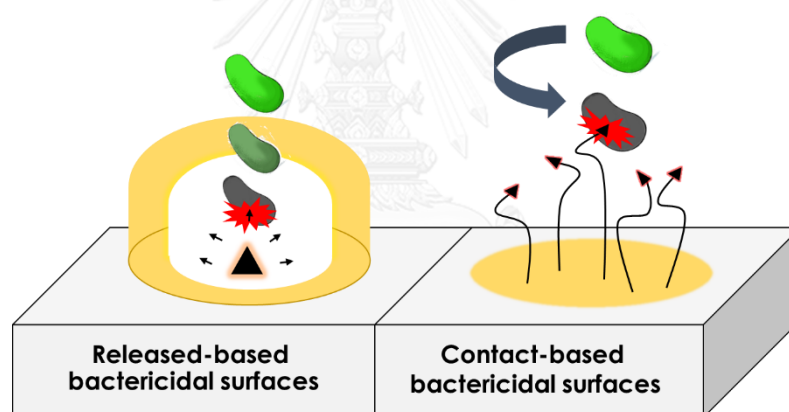


**Figure 1.2** Antibacterial mechanism of released-based (left) and contact-based (right) bactericidal surfaces [1].

For contact-based bactericidal surfaces, antibacterial agents are permanently immobilized on surfaces by either physical adsorption or covalent conjugation. Biocidal agents do not release to the surrounding, so the sufficiently high biocide concentration will kill bacteria upon contact. The biocidal agents can be either small molecules or natural biomolecules [4, 8-12].

#### 1.4 Antibacterial cellulose

Antibacterial surfaces from various substances such as gold [13], glass [14], cellulose [8, 9, 11, 15], polyurethane [16] and other polymer have been studied from researchers around the world. In this regards, cellulose has been one of the most widely used materials due to its biocompatible and biodegradable properties.

Cellulose is the most abundant and renewable polymer resource. It is biosynthesized by living organisms ranging from higher to lower plant and some bacteria [10]. As pointed out in **Figure 1.3**, cellulose is a linear homopolymer consisting of  $\beta$ -1,4-glycosidic linked D-anhydroglucopyranose units [17]. Each monomer contains three hydroxyl groups. These hydroxyl groups have abilities to form both intra- and intermolecular hydrogen bonds in its structure resulting in the crystalline packing and other physical properties of cellulose [18]. Moreover, the multiple free hydroxyl groups can be used as a precursor for chemical modifications. We will focus on the covalently modification of cellulose derivatives for contact-based bactericidal surfaces.

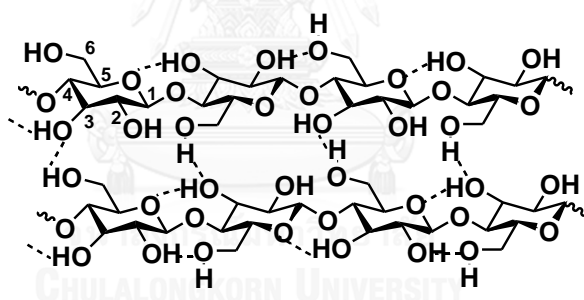


**Figure 1.3** Chemical structure of cellulose [17, 18].

Various amino-containing molecules have been used to modify antibacterial surfaces due to its positive charges. These positive charges can be either permanent or pH-dependent. Quaternary ammonium compounds (QACs) contain permanently positive charges with the structure  $NR_4^+$ , R being an alkyl group or an aryl group. Primary, secondary or tertiary ammonium cations are positively charged by protonation in the solution with pH lower than its pKa. These positive charges can interact with the negatively charged components of both Gram-positive and Gram-negative bacteria through electrostatic interactions. The binding occurs with lipoteichoic acid in Gram-positive bacterial membrane and lipopolysaccharides in Gram-negative bacterial

membrane [3, 19, 20]. These interference will disrupt the membrane integrities and cause cell death.

QACs parent units with lipophilic adjuncts were reported by the Abel group [8]. Appropriate haloalkanes ( $R = C8 - C18$ ) were reacted with 1,4-Diazabicyclo [2.2.2]octane (DABCO) and resulted in monocationic DABCO derivatives. These monocationic salts were immobilized on cotton and filter paper in two steps as shown in **Figure 1.4**. Surface modifications of the DABCO surface with an alkyl group with varying length from C10 to C18 illustrated strong antibacterial activities against three species of Gram-positive bacteria. Interestingly, **DABCO-C16** surfaces showed 100% inhibition on both Gram-positive and Gram-negative bacteria.

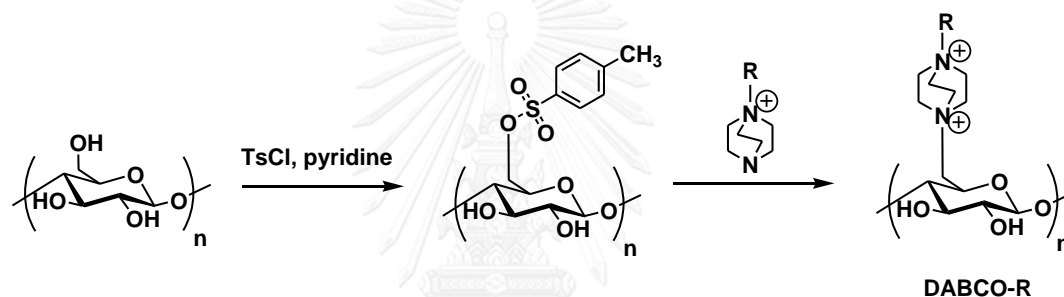


**Figure 1.4** Synthetic scheme of DABCO-R surfaces ( $R$  vary from C8 to C18) [8].

Moreover, DABCO derivatives can also be appended on methyl  $\alpha$ -D-glucopyranoside [21] as shown in **Figure 1.5**. DABCO-C18 modified surface, **Compound 12**, revealed only 1% growth of *Staphylococcus aureus* on the surface. In contrast, DABCO-C16 modified surface did not show high bacterial growth inhibition. The minimum inhibitory concentration (MIC) was higher than  $10^4 \mu\text{M}$ .

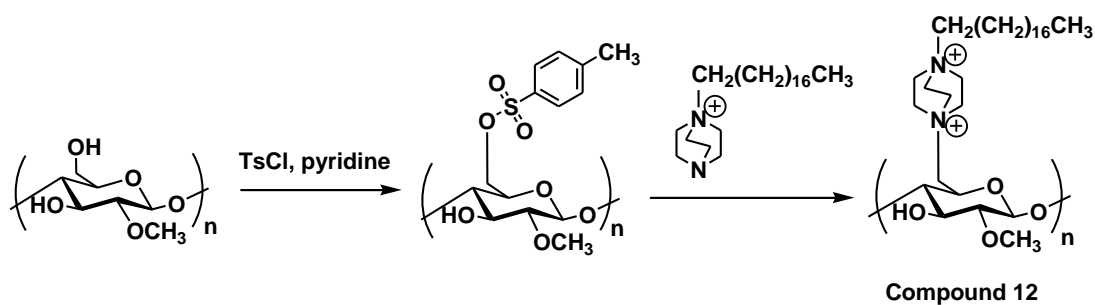


**Figure 1.5** Synthetic scheme of DABCO derivative modified methyl  $\alpha$ -D-glucopyranoside [21].

Polyethyleneimine (PEI) have also been used as a QACs parent unit for modifications of common woven textiles such as cotton, wool, nylon, and polyester by the Lin group [15]. Firstly, cotton with hydroxyl groups and wool with amino groups were modified with 4-bromobutyryl chloride as shown in **Figure 1.6**. PEI with different molecular weight were *N*-alkylated and subsequently modified with bromohexane and iodomethane. The textiles prepared using 750-kDa PEI showed a broad antibacterial spectrum against *Staphylococcus aureus*, *Staphylococcus epidermidis*, *Escherichia coli*, *Pseudomonas aeruginosa* and also fungi. For antimicrobial textile applications, soapy washing was applied to *N*-alkylated PEIs modified cotton. PEIs with molecular weight less than 2 kDa modified cotton revealed significant reduction of antibacterial potencies. However, the potencies of 25-kDa and 750-kDa PEIs modified cotton remained after the second washing. The dependence of antibacterial activities on the molecular weight of PEIs was confirmed by modifying non-porous material,  $\text{NH}_2$ -glass slides, with the same method. After washing off, 750- and 25-kDa PEIs modified surfaces showed high antibacterial activities. In contrast, their 2- and 0.8-kDa counterparts did not.

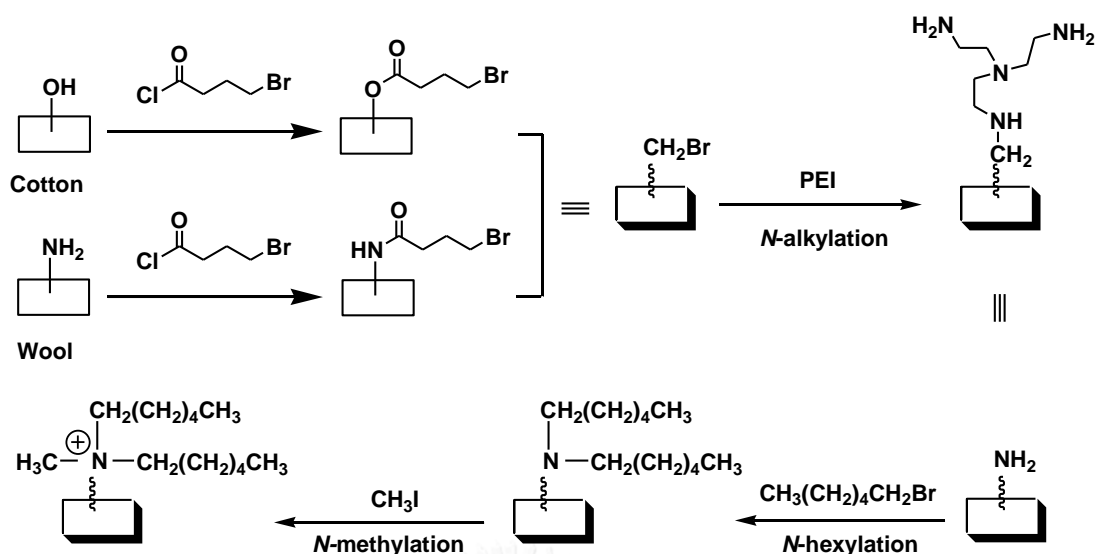
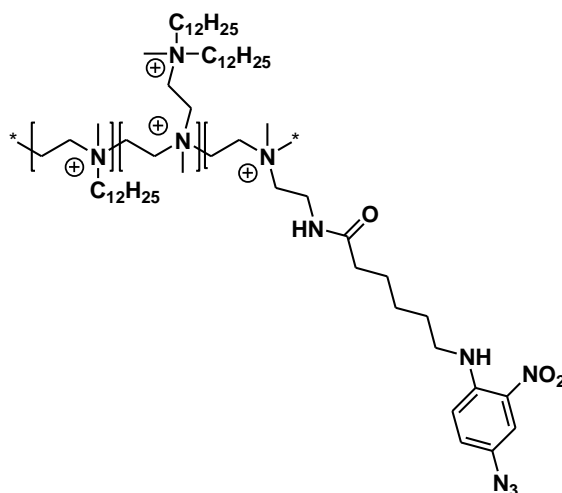


Figure 1.6 Synthetic scheme of PEI derivatives modified cotton and wool [15].

Modified cotton using branched PEI (molecular weight of 750 kDa) with hydrophobic and cationic portions was also studied by the Hsu group [22]. Dodecyl chains and hexanoyl chain containing aryl azide were attached to amino groups of PEI, followed by quaternization using iodomethane. The structure of *N,N,N*-ANPAH, dodecyl, methyl-PEI are shown in **Figure 1.7**. After dipping cotton into the solution of this polymer in dichloromethane, followed by irradiation of both sides of cellulose at 365 nm, the photosensitive aryl azide moiety became more reactive toward cellulosic hydroxyl groups. The covalently modified cotton showed high bactericidal efficiencies against *Staphylococcus aureus* and *Escherichia coli*.



**Figure 1.7** Molecular structure of *N,N,N*-ANPAH, dodecyl, methyl-PEI [22].

Not only the long alkyl chains can perform antibacterial activities, but a propyl chain can also function in the same way. Antibacterial properties of modified cellulose using a propyl chain with terminal QAC were studied by Chaker and Boufi [9]. As shown in **Figure 1.8**, glycidyl trimethyl ammonium chloride (GMA) was immobilized on nanofibrillar cellulose (NFC) through nucleophilic addition of hydroxyl groups of cellulose to the epoxide ring of GMA. C-NFC nanocomposite gel was prepared by using polyvinyl alcohol (PVA) as a matrix. The C-NFC/PVA gel increased visible transmittance due to the fact that the positive charge on C-NFC induces electrostatic repulsion. The C-NFC/PVA was casted into petri dishes and tested for antibacterial activities against both Gram positive and Gram negative bacteria. The C-NFC/PVA film demonstrated great antibacterial inhibitions with no colony growing on the film.

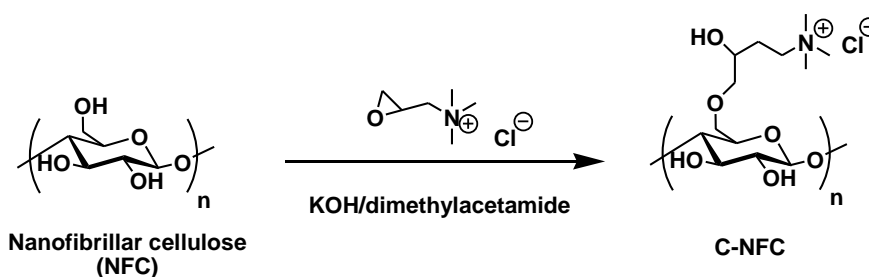


**Figure 1.8** Synthetic scheme of GMA modified nanofibrillar cellulose [9].

Furthermore, a propyl chain with terminal free amino groups can also exhibit high antibacterial activities as well. 3-aminopropyltrimethoxysilane (APS) grafting on bacterial cellulose (BC) was reported by the Fernandes group [10]. The simple reaction can be performed in acetone as shown in **Figure 1.9**. The acetone induced reaction was occurred by an imine formation between carbonyl groups of acetone and amino groups of APS (shown in **Figure 1.10**) [23]. The second phase, the hydrolysis of methoxy groups occurred and silanol groups were produced. Finally, these silanol groups were condensed with hydroxyl groups of cellulose to form Si-O-C bond and also condensed with each other to form siloxane. Antibacterial activities of **BC-NH<sub>2</sub>** against *Staphylococcus aureus* and *Escherichia coli* showed more than three log reduction of bacterial growth. They described the antibacterial mechanism that the terminal amino group of **BC-NH<sub>2</sub>** can provide a polycationic structure by being protonated. The positive charge affected an interaction with the cytoplasmic membrane of bacteria resulting in significant antibacterial activities. Moreover, **BC-NH<sub>2</sub>** displayed high biocompatibility with human adipose derived stem cells (ADSCs) after 72 hours of contact.

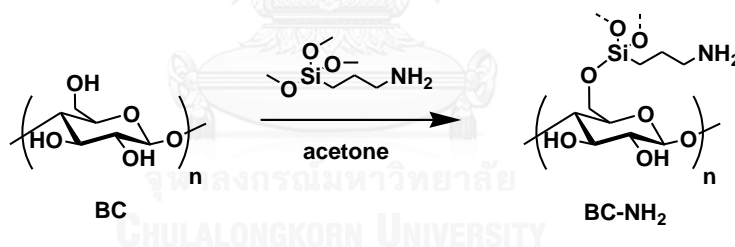


**Figure 1.9** Synthetic scheme of APS modified bacterial cellulose [10].



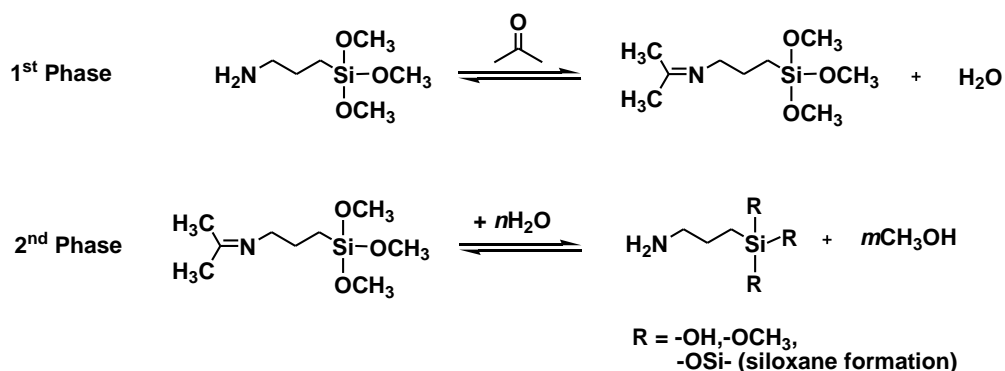


Figure 1.10 Mechanism of acetone induced polymerization of APS [23].

Using of diamino-containing molecules as spacer chains was studied by the Nakamura group [11]. The immobilization reactions of 1,3-diaminopropane and 4,7,10-trioxa-1,13-tridecanediamine (DA) on cotton surface are shown in **Figure 1.11**. Further modification on terminal amino groups with antimicrobial peptides (AMPs) were performed and the peptides-immobilized cotton exhibited high antibacterial activities against *Staphylococcus aureus* and methicillin-resistant *Staphylococcus aureus* (MRSA). In the aforementioned study, DA-modified cotton did not show any appreciable antibacterial activity. However, our preliminary results found that DA-modified cotton can inhibit bacterial growth on surfaces, prompting us to further investigate this class of compounds for their antibacterial activities.

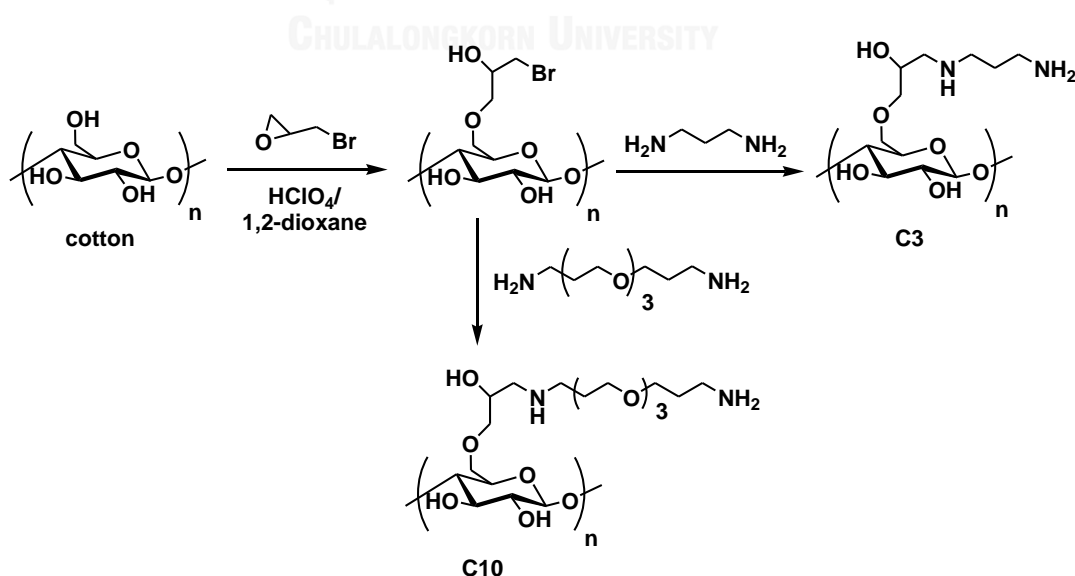


Figure 1.11 Synthetic scheme of diamino spacer chains modified cotton [11].

This study aimed to develop contact-based bactericidal surfaces by appending simple chemical scaffolds on cotton surface through covalent modifications. The antibacterial activities of four types of amino-containing molecules (3-aminopropyl-trimethoxysilane (**APS**), polyethyleneimine (**PEI**), 1,4-diazabicyclo[2.2.2]octane (**DABCO**), and 4,7,10-trioxa-1,13-tridecanediamine (**DA**) and its derivatives) will be studied. The knowledge obtained from these systematic studies would be beneficial for elucidating structure-activity relationship of this type of scaffolds on cotton surface, thereby leading to more efficient utilizations of this material in a variety of applications.

The objectives of this research are:

1. To develop simple methods for immobilizing various amino-containing molecules on cotton surfaces.
2. To evaluate antibacterial activities of the modified cotton surfaces against non-pathogenic bacteria and foodborne pathogens.
3. To evaluate the biocompatibility of the modified cotton surfaces against a mammalian cell line.

## CHAPTER II

### EXPERIMENT

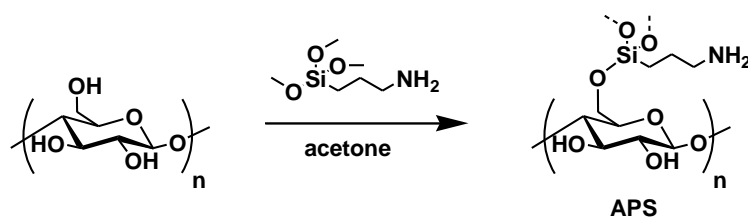
#### 2.1 Materials

All chemicals and reagents were purchased from Acros organics, Carlo Erba reagents S.p.A., Fluka, Merck, and Sigma-Aldrich Co., Ltd. All solvents were purchased from RCI Labscan (Thailand) and used without further purification. MilliQ water was obtained from ultrapure water system with Millipak<sup>®</sup> 40 filter unit 0.22  $\mu\text{m}$ , Millipore (USA). 100% cotton fabric was purchased from Thai Textile Development and Finishing Co., Ltd. and washed with *N,N*-dimethylformamide (DMF), deionized water, methanol and dichloromethane before use. *Staphylococcus aureus* (ATCC 6538P), *Escherichia coli* (ATCC 8739) and *Pseudomonas aeruginosa* (ATCC 9027) were cultured in HiMedia Nutrient Broth (NB). Foodborne pathogens including *Escherichia coli* (IAM 1264), *Listeria monocytogenes* (CIP 103575), *Salmonella enterica* subsp. *enterica* (ATCC 13311) and *Acinetobacter baumannii* (JCM 6841) were cultured in BBL<sup>™</sup> Trypticase<sup>™</sup> Soy Broth (TSB). *Leuconostoc carnosum* (JCM 9695) were cultured in Oxoid<sup>™</sup> de Man, Rogosa and Sharpe Broth (MRSB). L-929 mouse connective tissue fibroblast (DSMZ ACC 2) cell lines were cultivated in Roswell Park Memorial Institute medium (RPMI) with 10% Fetal Bovine Serum (FBS).

#### 2.2 Synthesis of amino-containing surfaces

##### 2.2.1 Synthesis of APS-modified surface (APS)

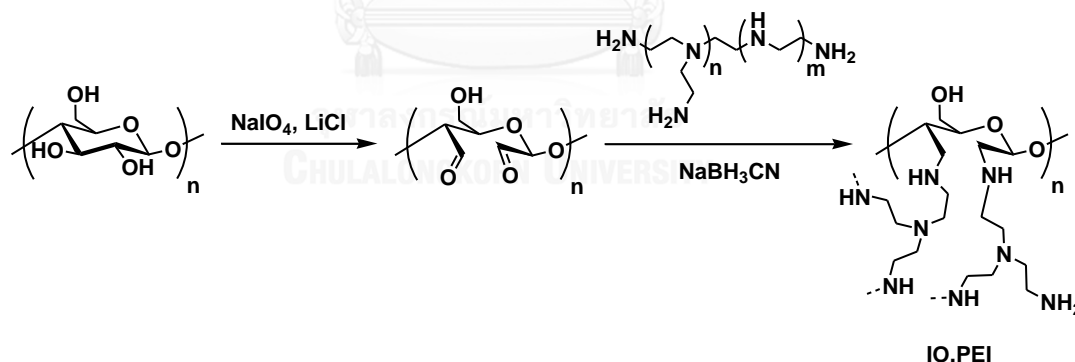
Cotton fabric (6.0 x 6.0 cm<sup>2</sup>) was immersed in a solution of 3-aminopropyltrimethoxysilane (APS) (1.0 mL, 0.52 M) in acetone (10.0 mL). The reaction was maintained at room temperature for 5 hours with 160-ppm shaking. The surface was then washed twice with acetone (5 minutes each) to remove unreacted residues and heated at 110 oC for 2 hours. After cooled down to room temperature, the surface was incubated in acetone for 18 hours and then air-dried.



**Scheme 2.1** Synthesis of APS-modified surface (APS).

### 2.2.2 Synthesis of $\text{IO}_4/\text{PEI}$ -modified surfaces (IO.PEI)

Cotton fabric ( $6.0 \times 6.0 \text{ cm}^2$ ) was shaken in a solution of sodium metaperiodate (86.0 mg, 0.04 M) and lithium chloride (0.89 g, 2.1 M) in Milli-Q water (10.0 mL) for 5 minutes. The surface was subsequently washed with deionized water (2x, 5 minutes each) and methanol (5 minutes). Next, the surface was shaken in a solution of polyethyleneimine (PEI; branched, 25 kDa) (260 mg, 1.6 mM) and sodium cyanoborohydride (1.26 mg, 2.0 mM) in 50% triethylamine in methanol (10.0 mL) at  $45^\circ\text{C}$  for 24 hours. The surface was washed twice with methanol (5 minutes each), deionized water (5 minutes), DMF (overnight) to remove unreacted residues, methanol (2x, 5 minutes each) and then air-dried.

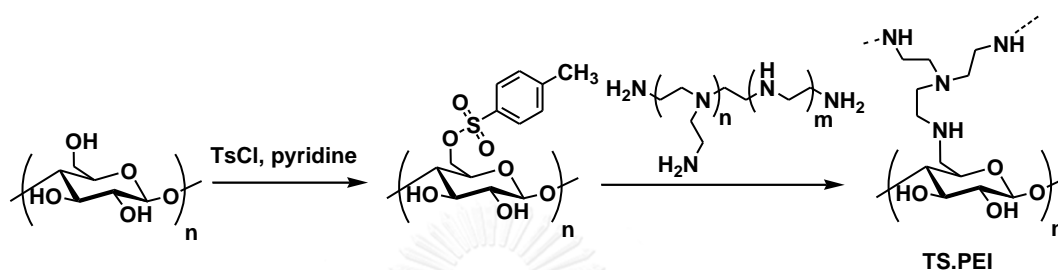


**Scheme 2.2** Synthesis of  $\text{IO}_4/\text{PEI}$ -modified surfaces (IO.PEI).

### 2.2.3 Synthesis of OTs/PEI modified surface (TS.PEI)

Firstly, cotton fabric ( $6.0 \times 6.0 \text{ cm}^2$ ) was reacted with *p*-toluenesulfonylchloride (3.82 g, 2.0 M) in pyridine (15.0 mL) for 90 minutes. After washing with DMF (2x, 5 minutes each), methanol (2x, 5 minutes each), dichloromethane (2x, 5 minutes each) and air-drying, the tosylated surface can be used

for further modification. This surface was shaken in a solution of PEI (0.40 g, 1.6 mM) in 15-mL DMF for 18 hours. Then, the surface was washed with 5.0 M sodium hydroxide in methanol (5 minutes), methanol (2x, 5 minutes each), DMF (5 minutes), deionized water (4x, 5 minutes each) and dried in an oven at 40°C for 10 hours. Finally, the surface was washed with DMF overnight to remove unreacted residues, methanol (2x, 5 minutes each) and then air-dried.



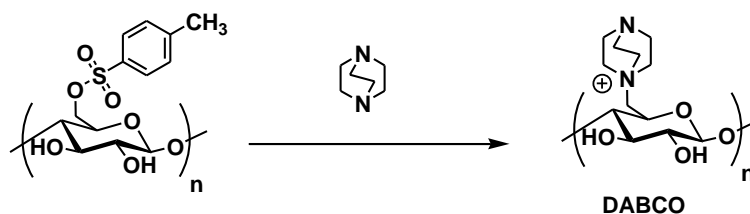
**Scheme 2.3** Synthesis of OTs/PEI modified surface (TS.PEI).

#### 2.2.4 Fabrication of physically-adsorbed PEI surface (Phys.PEI)

Cotton fabric (6.0 x 6.0 cm<sup>2</sup>) was shaken in a solution of PEI (0.40 g, 1.6 mM) in DMF 15.0 mL for 18 hours. After the reaction, the surface was washed with 5.0 M sodium hydroxide in methanol (5 minutes), methanol (2x, 5 minutes each), DMF (5 minutes), deionized water (4x, 5 minutes each) and dried in an oven at 40°C for 10 hours. Finally, the surface was washed with DMF overnight to remove unreacted residues, methanol (2x, 5 minutes each) and then air-dried.

#### 2.2.5 Synthesis of DABCO modified surface (DABCO)

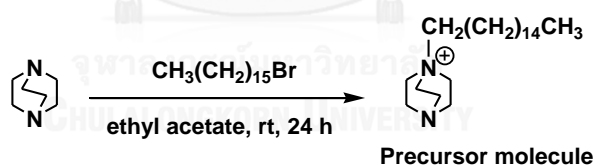
The tosylated surface was prepared using the same condition as in 2.2.3 and was then treated with a solution of 1,4-diazabicyclo[2.2.2]octane (DABCO) (0.45 g, 0.36 M) in 50% acetonitrile in dichloromethane (10.0 mL) for 18 hours. The reacted surface was washed with ethyl acetate (2x, 5 minutes each), methanol (5 minutes), acetonitrile (5 minutes) and dichloromethane (5 minutes), respectively.



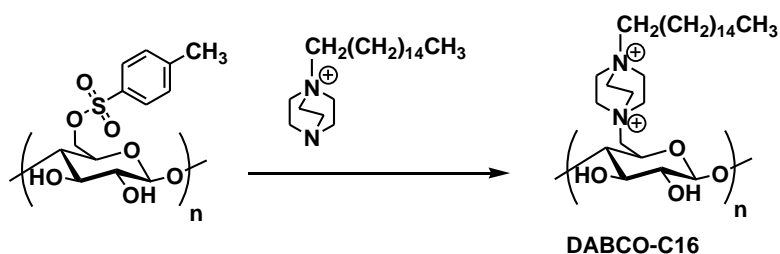
**Scheme 2.4** Synthesis of DABCO modified surface (DABCO).

### 2.2.6 Synthesis of DABCO-C16 modified surface (DABCO-C16)

The precursor molecule was first synthesized by reacting DABCO (10.0 g, 90 mmol) with 1-bromohexadecane (5.5 mL) in ethyl acetate (90 mL) (**Scheme 2.5**). After stirring at room temperature for 24 hours, white precipitate was obtained. The precipitate was filtered and washed with ethyl acetate and diethyl ether. The identity of the product was confirmed by  $^1\text{H}$  Nuclear Magnetic Resonance spectroscopy ( $^1\text{H}$  NMR, Varian Mercury+, 400 MHz). Next, the tosylated surface prepared by condition in **2.2.3** was shaken in a solution of the precursor molecule (1.5 g, 0.36 M) in 50% acetonitrile in dichloromethane (10.0 mL) for 18 hours and washed with ethyl acetate (2x, 5 minutes each), methanol (5 minutes), acetonitrile (5 minutes), dichloromethane (5 minutes) and hexane (5 minutes), respectively.



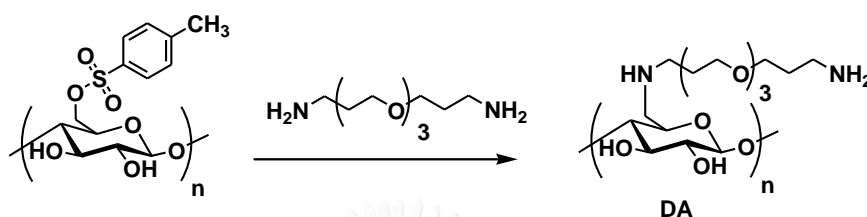
**Scheme 2.5** Synthesis of the precursor molecule for DABCO-C16 fabrication.



**Scheme 2.6** Synthesis of DABCO-C16 modified surface (DABCO-C16).

### 2.2.7 Synthesis of DA modified surface (DA)

The tosylated surface prepared by condition in 2.2.3 was immersed in a solution of 4,7,10-trioxa-1,13-tridecanediamine (3.5 mL, 1.0 M) in 15-mL DMF for 18 hours. The surface was washed with 5.0 M sodium hydroxide in methanol (5 minutes), methanol (2x, 5 minutes each), DMF (5 minutes), deionized water (4x, 5 minutes each) and dried in an oven at 40°C for 18 hours.



**Scheme 2.7** Synthesis of DA modified surface (DA).

Surface **DA** was further modified as follows.

#### A) Synthesis of DA.CO.C10

A solution of decanoic acid (19.0  $\mu$ L, 1.0 M), hydroxybenzotriazole (HOBt.H<sub>2</sub>O) (17 mg, 1.1 M), *N,N'*-diisopropylcarbodiimide (DIC) (17  $\mu$ L, 1.0 M) in anhydrous DMF (100  $\mu$ L) was spotted on surface **DA** for 2  $\mu$ L, the whole process was repeated two more times (10 minutes each). The surface was washed with DMF (2x, 5 minutes each), methanol (2x, 5 minutes each) and hexane (5 minutes).

#### B) Synthesis of DA.CO.C16

A solution of hexadecanoic acid (26.0 mg, 1.0 M), HOBt.H<sub>2</sub>O (17 mg, 1.1 M), DIC (17  $\mu$ L, 1.0 M) in anhydrous DMF (100  $\mu$ L) was spotted on surface **DA** for 2  $\mu$ L, the whole process was repeated two more times (10 minutes each). The surface was washed with DMF (2x, 5 minutes each), methanol (2x, 5 minutes each) and hexane (5 minutes).

#### C) Synthesis of DA.C10

Surface **DA** was immersed in a solution of 1-bromodecane (1.05 mL, 0.5 M), pyridine (805  $\mu$ L, 1.0 M) in 10-mL DMF. The reaction was kept shaking at room temperature for 20 hours. Then, the reacted surface was washed with DMF (2x,

5 minutes each), methanol (5 minutes), 0.1 M sodium chloride in deionized water (5 minutes), deionized water (5 minutes), methanol (5 minutes) and hexane (5 minutes), respectively.

#### **D) Synthesis of DA.C16**

Surface **DA** was immersed in a solution of 1-bromohexadecane (1.53 mL, 0.5 M), pyridine (805  $\mu$ L, 1.0 M) in 10-mL DMF. After shaking at room temperature for 20 hours, the surface was then washed with DMF (2x, 5 minutes each), methanol (5 minutes), 0.1 M sodium chloride in deionized water (5 minutes), deionized water (5 minutes), methanol (5 minutes) and hexane (5 minutes), respectively.

#### **E) Synthesis of DA.MeI**

Surface **DA** was shaken in a solution of iodomethane (310  $\mu$ L, 0.5 M) in 10-mL DMF at room temperature for 20 hours. After the reaction, the surface was washed with DMF (2x, 5 minutes each), methanol (5 minutes), 0.1 M sodium chloride in deionized water (5 minutes), deionized water (5 minutes) and methanol (5 minutes), respectively.

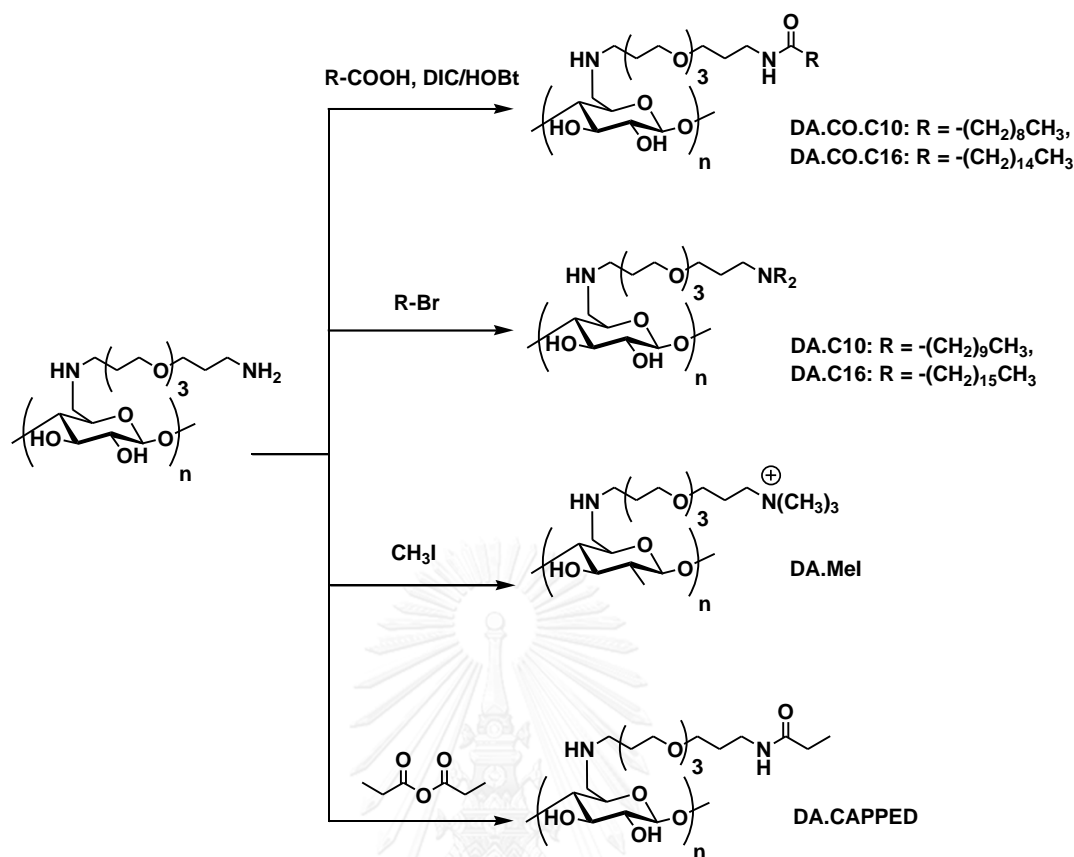
#### **F) Synthesis of DA.C10.MeI**

Surface **DA.C10** was shaken in a solution of iodomethane (310  $\mu$ L, 0.5 M) in 10-mL DMF at room temperature for 20 hours. After the reaction, the surface was washed with DMF (2x, 5 minutes each), methanol (5 minutes), 0.1 M sodium chloride in deionized water (5 minutes), deionized water (5 minutes) and methanol (5 minutes), respectively.

#### **G) Synthesis of DA.CAPPED**

Surface **DA** was shaken in a solution of 5% propionic anhydride in 10-mL DMF at room temperature for 15 minutes. The surface was then washed with DMF (2x, 5 minutes each), methanol (2x, 5 minutes each) and then air-dried.





Scheme 2.8 Further modifications of surface DA with additional reagents.

## 2.3 Characterization

### 2.3.1 Primary amine loading quantification by CI acid orange 7

2.5 x 2.5 cm<sup>2</sup> samples were immersed in a solution of CI acid orange 7 (25.0 mg, 1.4 M), acetic acid (475  $\mu\text{L}$ ) in 50-mL deionized water at 50 °C for 30 minutes. Each sample was washed several times with water (3 minutes each) and placed in 25% aqueous pyridine solution (1.0 mL) for 15 minutes. Absorbance of the solution was measured at 485 nm using Cary 100 Bio UV-Visible spectrophotometer.

### 2.3.2 Quaternary amine loading quantification by fluorescein sodium salt

2.0 x 2.0 cm<sup>2</sup> samples were immersed in 1% aqueous solution of fluorescein sodium salt (1.0 mL) for 5 minutes. Each sample was washed several times with deionized water (3 minutes each) and placed in 0.25% aqueous solution of cetyltrimethylammonium bromide (CTAB) (5.0 mL) for 15 minutes. The solution was

diluted with a 0.1 M aqueous phosphate buffer (pH 8.0) and measured for absorbance at 501 nm.

### 2.3.3 Attenuated Total Reflection Fourier Transform Infrared Spectroscopy (ATR-FTIR)

ATR-FTIR spectra were obtained using a Thermo Scientific™ Nicolet™ iS™5 FT-IR spectrometer. The spectra were taken in transmittance mode over the wavenumber range of 400 – 4000  $\text{cm}^{-1}$ .

### 2.3.4 X-ray Photoelectron Spectroscopy (XPS)

XPS results were evaluated using PHI 5000 VersaProbe II (S) with an Al  $K\alpha$  ( $h\nu = 1486.6$  eV) source at a power of 100W (20 kV). The pass energy of wide spectra was 280 eV and for spectra from individual elements were 26 eV (C 1s), 55 eV (O 1s), 140 eV (N 1s), 224 eV (Si 2p, Br 3d). Most spectra were collected at an emission angle 45 degree from sample surface.

### 2.3.5 Scanning Electron Microscopy (SEM)

Surface morphology of unmodified and modified cotton was observed by SEM using a JEOL JSM-6480LV scanning electron microscope. Dried samples were deposited on a metal stub and coated with gold layer before an observation. The accelerating voltage used was 5 kV. Electron micrographs of the sample were recorded at different magnifications, ranging from 500x to 5000x.

## 2.4 Antibacterial activity assays

Antibacterial activities of all surfaces were tested against *Staphylococcus aureus* (ATCC 6538P), *Escherichia coli* (ATCC 8739) and *Pseudomonas aeruginosa* (ATCC 9027). The bacterial pre-inoculum cultures were grown under the condition as shown in **Table 2.1** with continuous shaking at 200 ppm and diluted to  $1 \times 10^7$  CFU/mL with 0.85% Normal Saline Solution (NSS). Samples ( $1.0 \times 1.0 \text{ cm}^2$ ) were placed in 12-well plates. 100  $\mu\text{L}$  of bacterial suspension was dropped on each sample and then incubated at 37 °C for 18 hours. After reaching the desired time period, the suspension was diluted into 10-mL NSS and serially diluted to  $10^{-4}$  folds. All dilutions were spotted

on agar plates and incubated at 37 °C until bacterial colonies were visible. Colony Forming Unit (CFU) of bacteria was counted and calculated to the number of bacterial growth on surfaces and the percentage of inhibition by using unmodified cotton as a negative control.

**Table 2.1** Strains and culture conditions of bacteria.

Pathogens	Strain	Medium	Incubated temperature
<i>Staphylococcus aureus</i>	ATCC 6538P	NB	37 °C
<i>Escherichia coli</i>	ATCC 8739	NB	37 °C
<i>Pseudomonas aeruginosa</i>	ATCC 9027	NB	37 °C

## 2.5 Inhibitory activities against foodborne pathogens

Inhibitory activities of various modified surfaces were tested against foodborne pathogens including *Escherichia coli* (IAM 1264), *Listeria monocytogenes* (CIP 103575), *Salmonella enterica* subsp. *enterica* (ATCC 13311), *Acinetobacter baumannii* (JCM 6841) and *Leuconostoc carnosum* (JCM 9695). The culture conditions were displayed in **Table 2.2**. The pathogens from stock cultures were incubated for 24 hours under optimum conditions. The pre-inoculum cultures were prepared by transferring 10- $\mu$ L solution to 10-mL medium and incubating for 24 hours. The solution was serially diluted with 0.85% NSS to  $10^{-8}$  folds. The suspension (100  $\mu$ L) from  $10^{-6}$  to  $10^{-8}$  dilutions were spread on agar plates, incubated and counted for CFU. 100- $\mu$ L suspension of  $10^{-2}$  dilution was dropped on each sample in 24-well plates and incubated for 18 hours. After reaching the desired time period, the suspension was diluted into 10-mL NSS and serially diluted to  $10^{-3}$  folds. All dilutions were spread on agar plates and incubated until bacterial colonies were visible, which was then followed by CFU counting. The inhibitory activities were calculated by using unmodified cotton as a negative control.

**Table 2.2** Strains and culture conditions of foodborne pathogens.

Pathogens	Strain	Medium	Incubated temperature
<i>Escherichia coli</i>	IAM 1264	TSB	37 °C
<i>Listeria monocytogenes</i>	CIP 103575	TSB	30 °C
<i>Salmonella enterica</i> subsp. <i>enterica</i>	ATCC 13311	TSB	37 °C
<i>Acinetobacter baumannii</i>	JCM 6841	TSB	30 °C
<i>Leuconostoc carnosum</i>	JCM 9695	MRSB	30 °C

## 2.6 Cytotoxicity assay

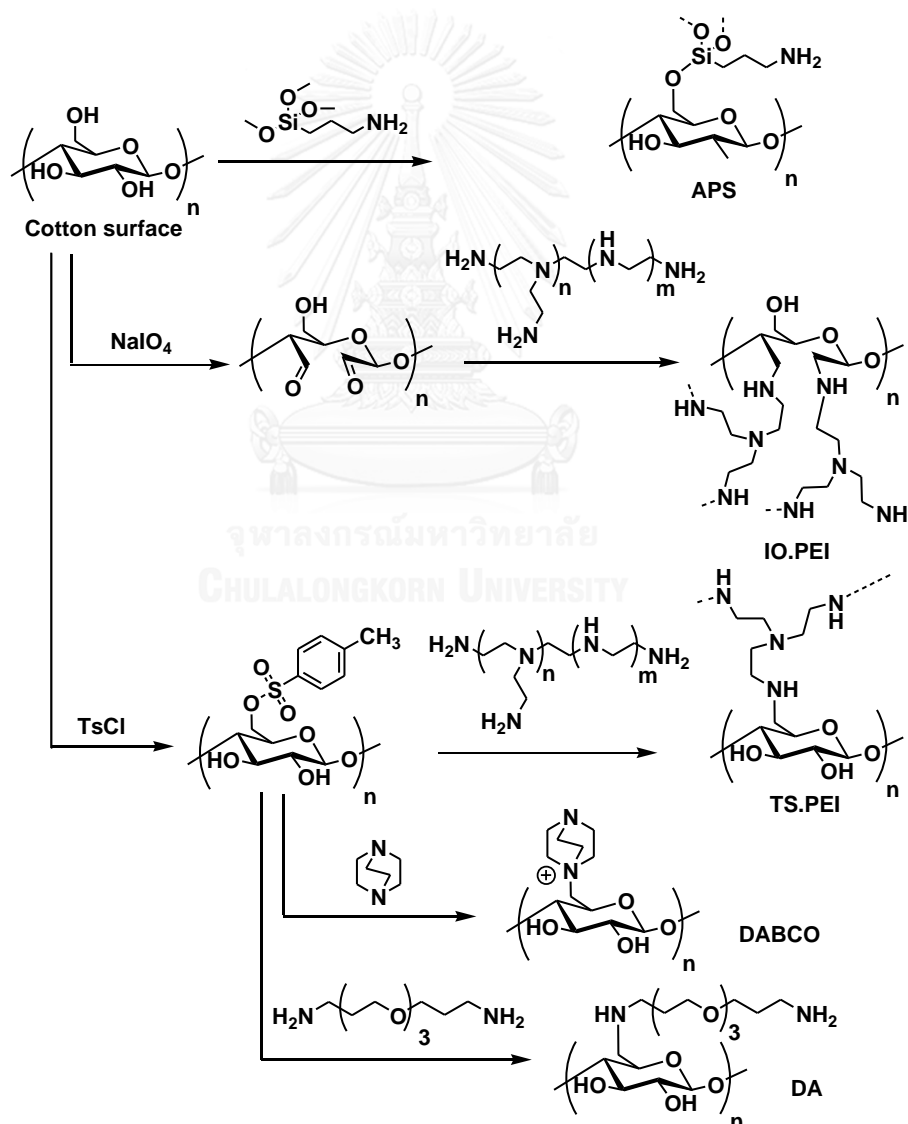
L-929 mouse connective tissue fibroblast (DSMZ ACC 2) cell line was cultivated in Roswell Park Memorial Institute (RPMI) medium with 10% Fetal Bovine Serum (FBS) at 37 °C in 5% CO<sub>2</sub> humidified atmosphere. All cotton samples were sterilized by immersing in 70% ethanol overnight. After air-dried, samples were placed in 24-well plates and 50 µL of L-929 fibroblast cells (4x10<sup>5</sup> cells/mL) was pipetted onto each sample and the soaked fabrics were incubated for 2 hours. 500 µL of RPMI medium was subsequently added to each well, and the solution was transferred for further incubation for 24 hours. Thereafter, 300 µL of 0.5 mg/mL MTT (3-(4,5-dimethylthiazol-2-yl)-2,5-diphenyltetrazolium bromide) in 0.9% NSS was added. The solution was further incubated for 2 hours, and was then added with 300-µL DMSO to dissolve formazan. The viability was determined by measuring 540-nm absorbance using Multiskan FC microplate reader.

## CHAPTER III

### RESULTS AND DISCUSSION

#### 3.1 Synthesis of amino-containing surfaces

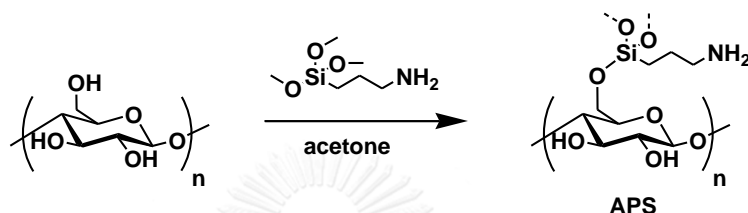
Four main types of amino-containing molecules including 3-aminopropyltrimethoxysilane (APS), polyethyleneimine (PEI), 1,4-diazabicyclo [2.2.2]octane (DABCO), 4,7,10-trioxa-1,13-tridecanediamine (DA) were immobilized on cotton surfaces via various chemical reactions (Scheme 3.1). The details of each reaction are described below.



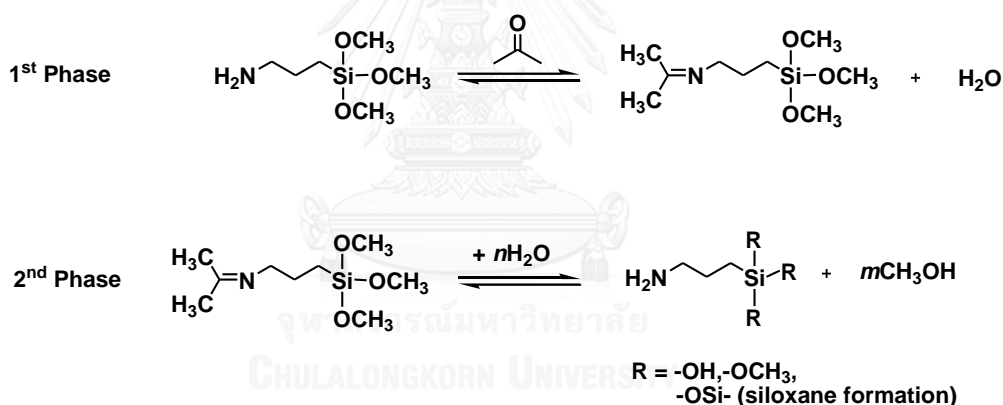
Scheme 3.1 Chemical grafting of amino-containing molecules onto cotton surfaces.

### 3.1.1 Synthesis of APS-modified surface (APS)

Surface APS was modified via the chemical reaction as shown in **Scheme 3.2**. An acetone induced reaction was occurred by an imine formation between carbonyl groups of acetone and amino groups of APS, followed by hydrolysis of methoxy groups and production of silanol groups [23]. Finally, these silanol groups were condensed with hydroxyl groups of cellulose and also condensed with each other to form polymeric siloxane (**Scheme 3.3**).



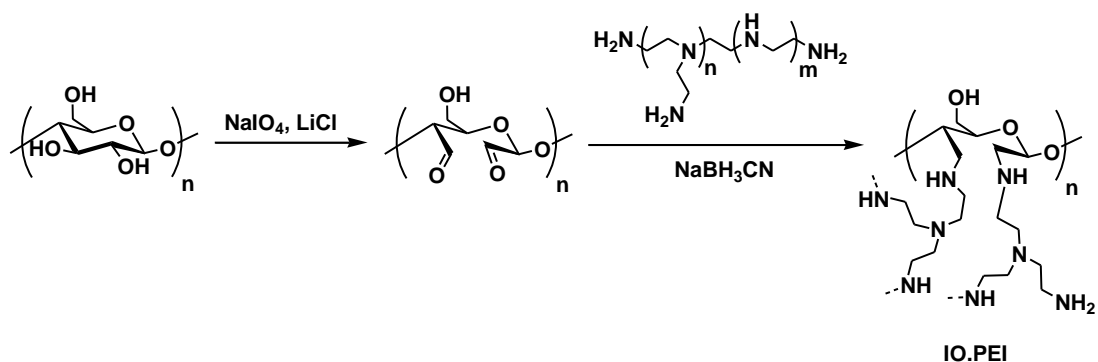
**Scheme 3.2** Synthesis of APS-modified surface (APS).



**Scheme 3.3** Mechanism of acetone-induced polymerization [23].

### 3.1.2 Synthesis of IO4/PEI-modified surfaces (IO.PEI)

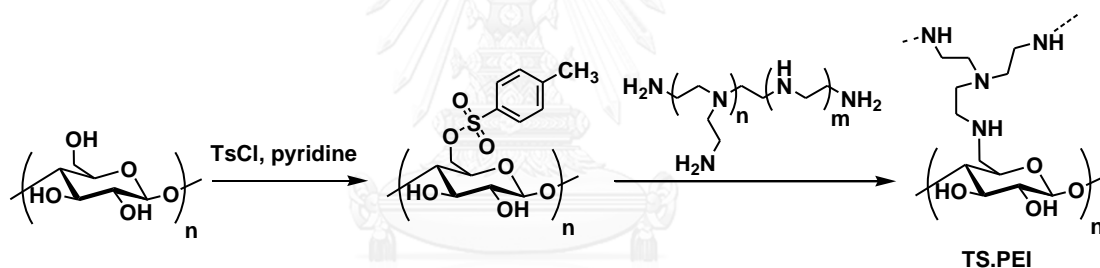
IO.PEI was modified using two steps as shown in **Scheme 3.4**. First, hydroxyl groups of cellulose were oxidized to dialdehyde groups, followed by reductive amination between the dialdehyde groups and amino groups of PEI.



**Scheme 3.4** Synthesis of IO4/PEI-modified surfaces (IO.PEI).

### 3.1.3 Synthesis of OTs/PEI modified surface (TS.PEI)

TS.PEI was modified via two step synthesis (**Scheme 3.5**). First, the hydroxyl group of cellulose was converted to the tosyl group, which is a good leaving group. The tosyl group was later reacted with amino groups of PEI in  $S_N2$  manner.



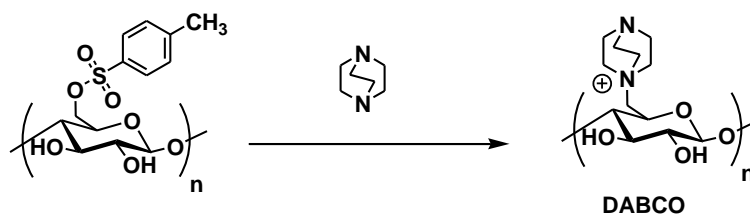
**Scheme 3.5** Synthesis of OTs/PEI modified surface (TS.PEI).

### 3.1.4 Fabrication of physically-adsorbed PEI surface (Phys.PEI)

Phys.PEI was created by simply immersing cotton surface in PEI solution. This adsorption was found to be relatively strong since DMF washing for overnight could not remove the molecule, likely because of strong hydrogen bonding.

### 3.1.5 Synthesis of DABCO modified surface (DABCO)

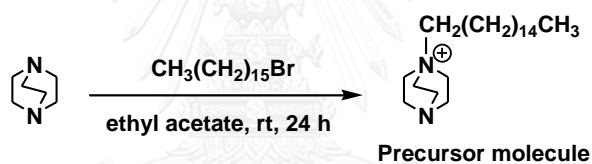
DABCO was synthesized by modifying the tosylated surface with DABCO as shown in **Scheme 3.6**. This surface exhibits a permanent single positive charge.



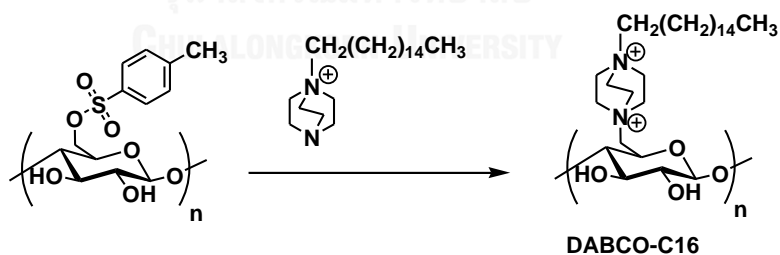
Scheme 3.6 Synthesis of DABCO modified surface (DABCO).

### 3.1.6 Synthesis of DABCO-C16 modified surface (DABCO-C16)

To fabricate the surface **DABCO-C16**, the precursor molecule was synthesized by reacting DABCO with 1-bromohexadecane in ethyl acetate for 24 hours (Scheme 3.7). After filtration to obtain a solid product, the solid was confirmed to be the desired product by  $^1\text{H}$  NMR spectrum (Figure A1). The compound was grafted onto the tosylated surface as shown in Scheme 3.8 to result in a new surface **DABCO-C16**, which has a permanent doubly positive charge in its structure.



Scheme 3.7 Synthesis of the precursor molecule for DABCO-C16 fabrication.



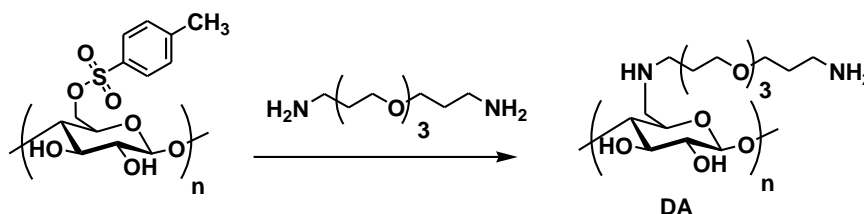
Scheme 3.8 Synthesis of DABCO-C16 modified surface (DABCO-C16).

### 3.1.7 Synthesis of DA modified surface (DA)

DA was synthesized by reacting the tosylated surface with 4,7,10-trioxa-1,13-tridecanediamine in an  $\text{S}_{\text{N}}2$  manner as shown in Scheme 3.9. As there are two amino groups on each terminus of the structure, 4,7,10-trioxa-1,13-tridecanediamine



can be used as a spacer. The further modifications on the terminal amino group with additional reagents were studied as shown in **Scheme 3.10**.



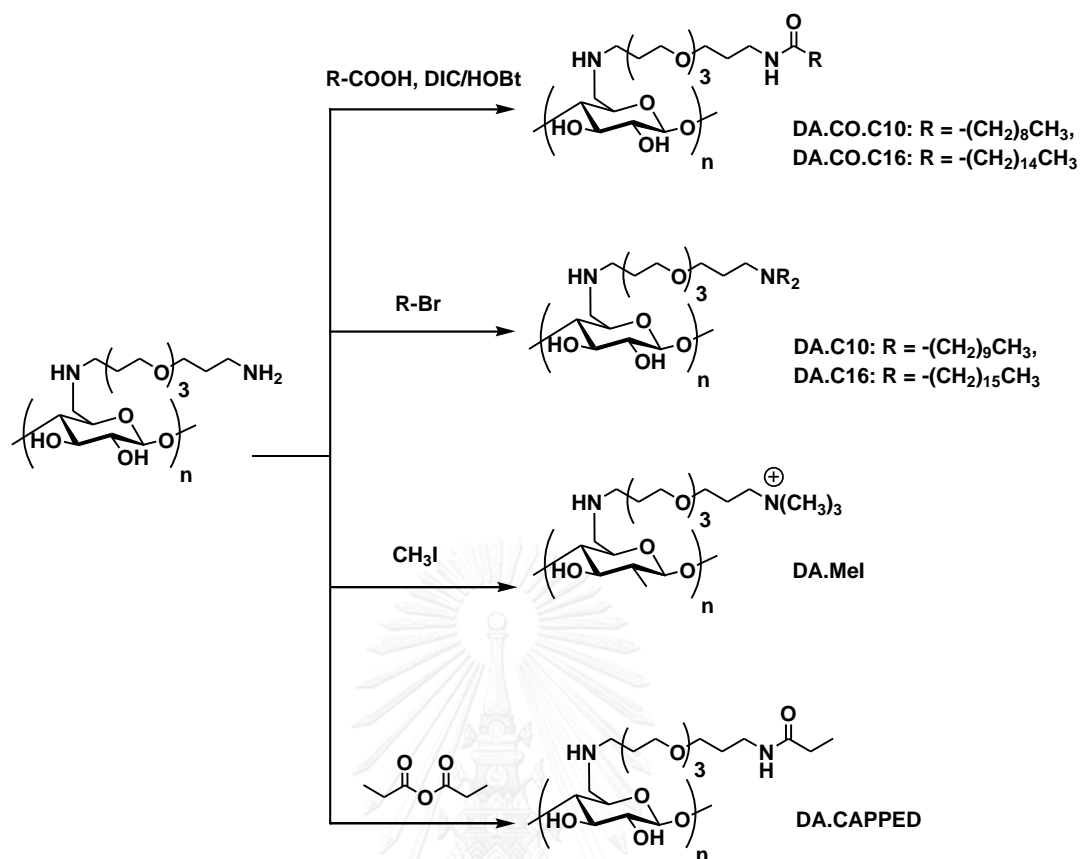
**Scheme 3.9** Synthesis of DA modified surface (DA).

**DA.CO.C10** and **DA.CO.C16** were synthesized by modifying **DA** with fatty acid chains (decanoic acid and hexadecanoic acid) via a standard carbodiimide coupling with diisopropylcarbodiimide (DIC) and hydroxybenzotriazole (HOBt). The introduction of the fatty acid chains aimed to fabricate a hydrophobic part on surface **DA**.

**DA.C10** and **DA.C16** were synthesized by modifying **DA** with alkyl bromides (1-bromodecane and 1-bromohexadecane) via alkylation ( $S_N2$ ). These modifications also aimed to increase hydrophobic properties of **DA**.

**DA.MeI** was synthesized by quaternizing **DA** with iodomethane, which is an active alkylating agent. This modification was expected to create a permanent positive charge on **DA**.

**DA.CAPPED** was synthesized by reacting **DA** with propionic anhydride. The propionyl group can protect free amino groups of **DA** from protonation and other reactions.



Scheme 3.10 Further modifications of surface DA with additional reagents.

### 3.2 Characterization

Both physical properties and chemical properties of surfaces were determined as follows.

#### 3.2.1 Primary amine loading quantification

Primary amine loading on unmodified and modified cotton surfaces was quantified using Cl acid orange 7 (the structure is shown in **Figure 3.1**) [11]. Cotton samples were first incubated in the dye solution under acidic condition, positive charges of protonated amino groups can interact with negative charges of the dye via the reversible electrostatic interaction [24]. After several washing with water, all samples were placed under basic condition, the positive charges of protonated amino groups become neutral and have no interaction with the dye, thus resulting in a release of the dye (if previously attracted). These solutions were used for UV measurement

and the loading was calculated. The molar extinction coefficient ( $\epsilon$ ) was determined to be  $16.328 \text{ mM}^{-1}\text{cm}^{-1}$  using the calibration curve as shown in **Figure 3.2**.

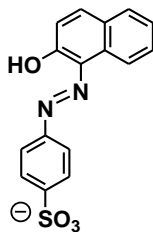


**Figure 3.1** Molecular structure of Cl acid orange 7.

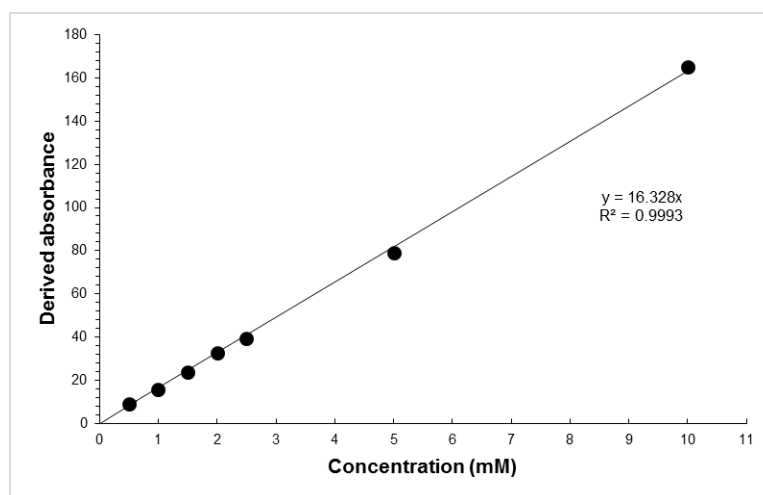


**Figure 3.2** Calibration curve of Cl acid orange 7 in 25% aq. pyridine solution.

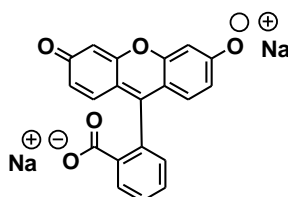
The primary amine loadings calculated from an average of three independent measurements are shown in **Table 3.1**. The highest value of **APS** indicated high efficiency of this immobilization reaction onto cotton surfaces through Si-O-C bond. Interestingly, **Phys.PEI** displayed high quantities of the amino loading although the interaction was merely non-specific physical adsorption between PEI and cotton. In fact, **TS.PEI** showed slightly less amount of the loading than **Phys.PEI**, suggesting that  $S_N2$  reaction did not improve the loading for PEI. On the other hand, this physical adsorption did not occur in **DA** without tosylation (denoted as **Phys.DA**). This was confirmed by significantly lower loading value of **Phys.DA**, compared to **DA**. The different amount of hydrogen bonding might affect the different physical adsorptions of PEI and DA on cotton surfaces.

**Table 3.1** Primary amine loading on surfaces.

Surfaces	Loading ( $\mu\text{moles}/\text{cm}^2$ )
Cotton	$0.0748 \pm 0.02$
APS	$0.5258 \pm 0.04$
TS.PEI	$0.3830 \pm 0.02$
Phys.PEI	$0.4149 \pm 0.02$
DA	$0.4110 \pm 0.06$
Phys.DA	$0.0821 \pm 0.01$

### 3.2.2 Quaternary amine loading quantification

Quaternary amine loading on unmodified and modified cotton surfaces was quantified using fluorescein sodium salt (the structure is shown in **Figure 3.3**) [15]. First, cotton samples were incubated in the dye solution, positive charges of quaternary amine can interact with negative charges of the fluorescein dye through the reversible electrostatic interaction. After several washes with water, treatment with a solution of cationic surfactant, cetyltrimethylammonium bromide (CTAB), resulted in a release of the dye (if previously attracted) into a solution. These solutions were used for UV measurement and the loading was calculated. The molar extinction coefficient ( $\epsilon$ ) was determined to be  $42.797 \text{ mM}^{-1}\text{cm}^{-1}$  using the calibration curve as shown in **Figure 3.4**.

**Figure 3.3** Molecular structure of fluorescein sodium salt.

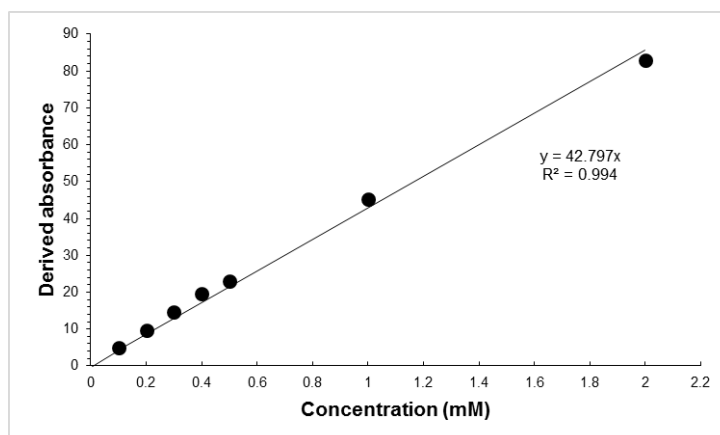


**Figure 3.4** Calibration curve of fluorescein sodium salt in 0.25% aq. CTAB.

The quaternary amine loadings calculated from an average of three independent measurements are shown in **Table 3.2**. The high quantities of **DABCO** indicated high efficiency of DABCO immobilization onto cotton surfaces. **DA** showed some amount of positive charges due to the protonation, however, this value could not be compared directly to the CI acid orange 7 method as it was not under acidic condition. **DA.MeI** showed the highest loading due to the reactivity of iodomethane. We hypothesized that **DA.C10** and **DA.C16** could not be quaternary amine due to the slow rate of  $S_N2$  reaction with these substrates. This hypothesis was further confirmed by quaternizing **DA.C10** with iodomethane. **DA.C10.MeI** displayed significant increase in loading.

**Table 3.2** Quaternary amine loading on surfaces.

Surfaces	Loading ( $\mu\text{moles}/\text{cm}^2$ )
Cotton	$0.0019 \pm 0.00$
DABCO	$0.3770 \pm 0.02$
DA	$0.2578 \pm 0.01$
DA.C10	$0.2382 \pm 0.01$
DA.C16	$0.2234 \pm 0.01$
DA.MeI	$0.5322 \pm 0.01$
DA.C10.MeI	$0.3373 \pm 0.01$

### 3.2.3 ATR-FTIR experiments

Functional groups of the unmodified and modified cotton surfaces were characterized using ATR-FTIR. Due to the fact that these modifications occurred mostly on the surface, and the amount of cellulose is extremely larger than the attached molecules, the characteristic peaks of cellulose thus dominated in all spectra as shown in **Figure 3.5**. Apart from the absorption bands of **cotton** at around  $3300\text{ cm}^{-1}$  (OH stretching) [10] and around  $2850\text{ cm}^{-1}$  ( $\text{CH}_2$  stretching) [10], the spectra of modified cotton (**APS**, **IO.PEI**, **TS.PEI**, **DABCO**) displayed two bands at around  $1650\text{ cm}^{-1}$  corresponding to  $\text{NH}_2$  deformation vibrations [25]. These  $\text{NH}_2$  vibrations can confirm the introduction of the amino-containing molecules onto cotton surfaces. Large changes were observed in the spectrum of **DABCO**. However, **DA** barely exhibited any changes. The physical properties of **DA** would be characterized using additional techniques.

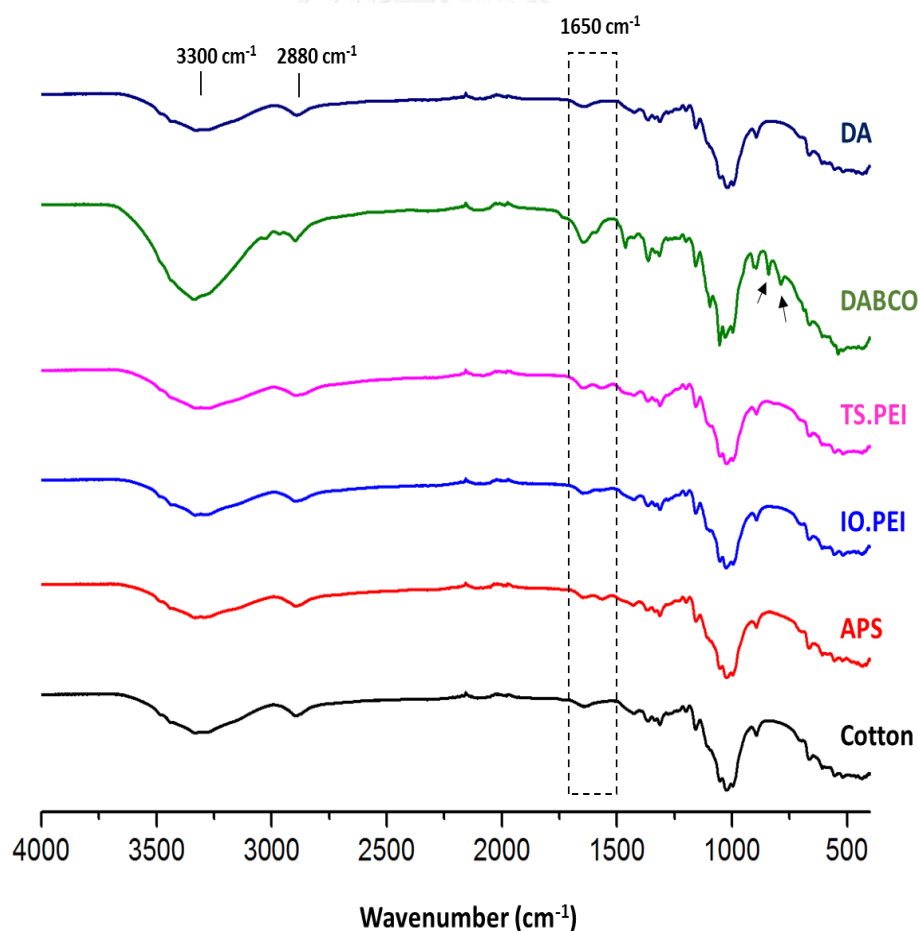


**Figure 3.5** ATR-FTIR spectra of unmodified and modified cottons.

### 3.2.4 Elemental compositions by XPS analysis

The elemental compositions of unmodified and modified cotton were studied by XPS analysis. Atomic concentration in **Table 3.3** and survey scan spectra in **Figure 3.6** showed significant quantities of carbon and oxygen in all samples. Trace of calcium was detected in some samples due to the manufacturer's washing procedure [22]. As expected, nitrogen content was significantly increased after modifications with amino-containing molecules. **APS** showed the highest content of nitrogen and silicon, whereas **DA** and **DA.CO.C10** displayed similar elemental compositions.

**Table 3.3** Atomic concentration (%) in survey scan spectra.

Surfaces	C1s	N1s	O1s	Si1p	Ca2p
Cotton	72.6	0.4	26.4	0.5	0.2
APS	62.4	1.8	33.4	2.1	0.3
DA	61.1	1.3	37.3	0.3	ND
DA.CO.C10	60.1	1.4	38.1	0.4	ND

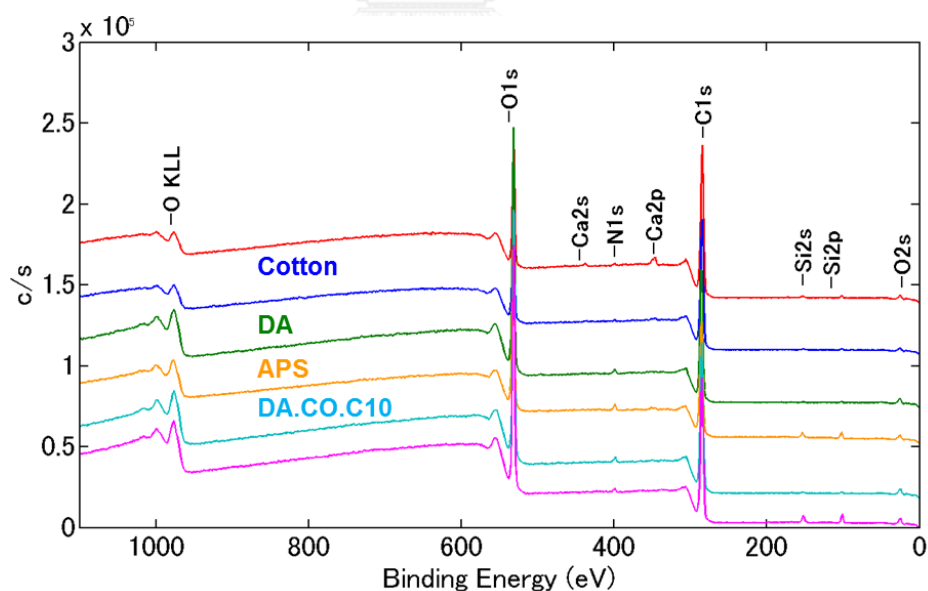


**Figure 3.6** XPS survey scan spectra of unmodified and modified cottons.

Curve fitting results of C1s as shown in **Figure 3.7** displayed the decreasing C-C, C-H ratios of **APS**, **DA** and **DA.CO.C10** comparing to **cotton** after the modifications. Interestingly, curve fitting results of N1s scan spectra as shown in **Figure 3.8** revealed that there are two peaks of N1s chemical state (denoted as N1s.cf1 and N1s.cf2) in **cotton**. After the amino modifications, the chemical state at 400.5 eV (N1s.cf3) were detected in **APS**, **DA** and **DA.CO.C10**.

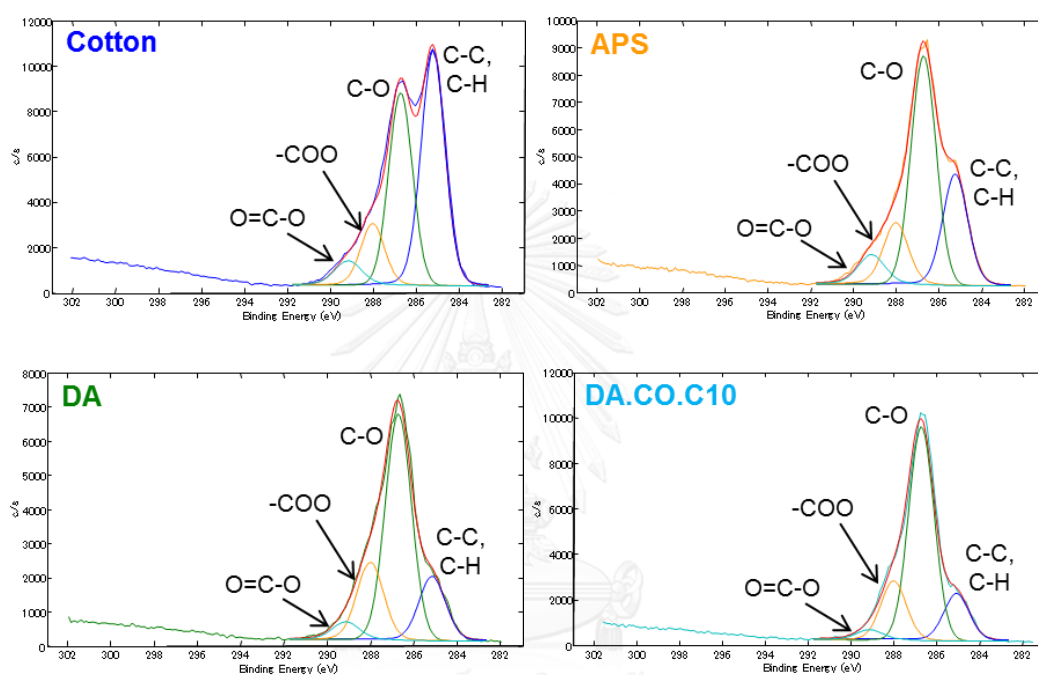


**Figure 3.7** Curve fitting results of C1s scan spectra.



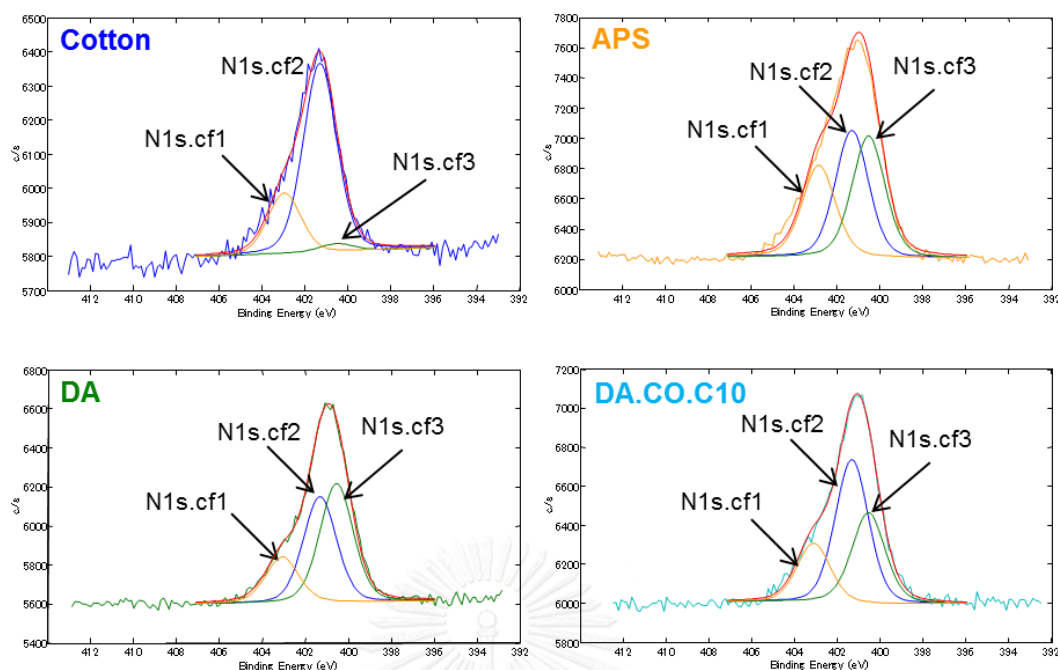


Figure 3.8 Curve fitting results of N1s scan spectra.

### 3.2.5 Surface morphology by SEM analysis

SEM analysis was carried out in order to study the morphological changes affected by chemical modifications. SEM images of unmodified and modified cottons with x500 and x5000 magnifications are shown in **Figure 3.9** and **3.10**, respectively. These images illustrated that the morphology of modified cotton were maintained after the chemical modification.

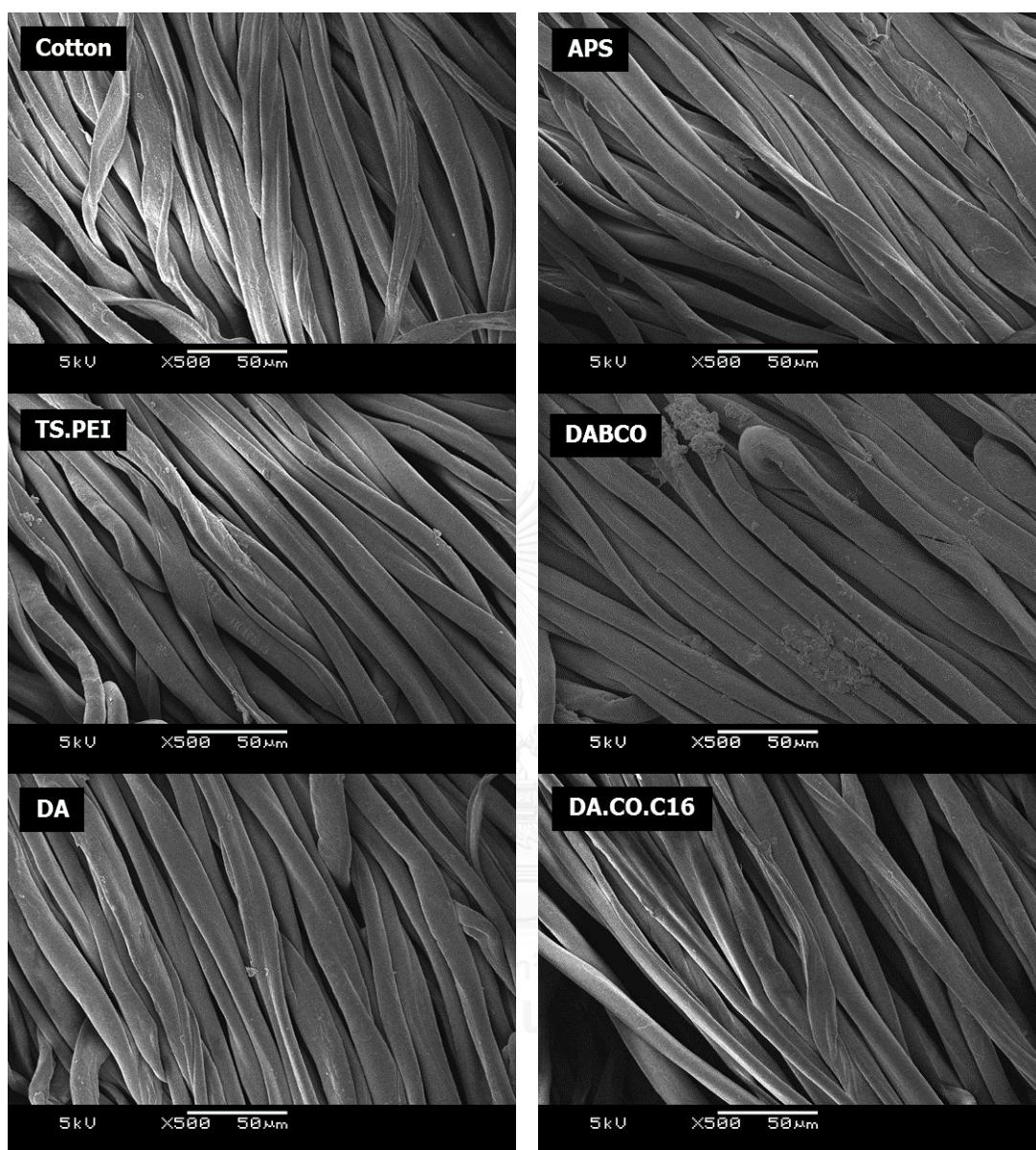


Figure 3.9 SEM images of unmodified and modified cotton with x500 magnification.

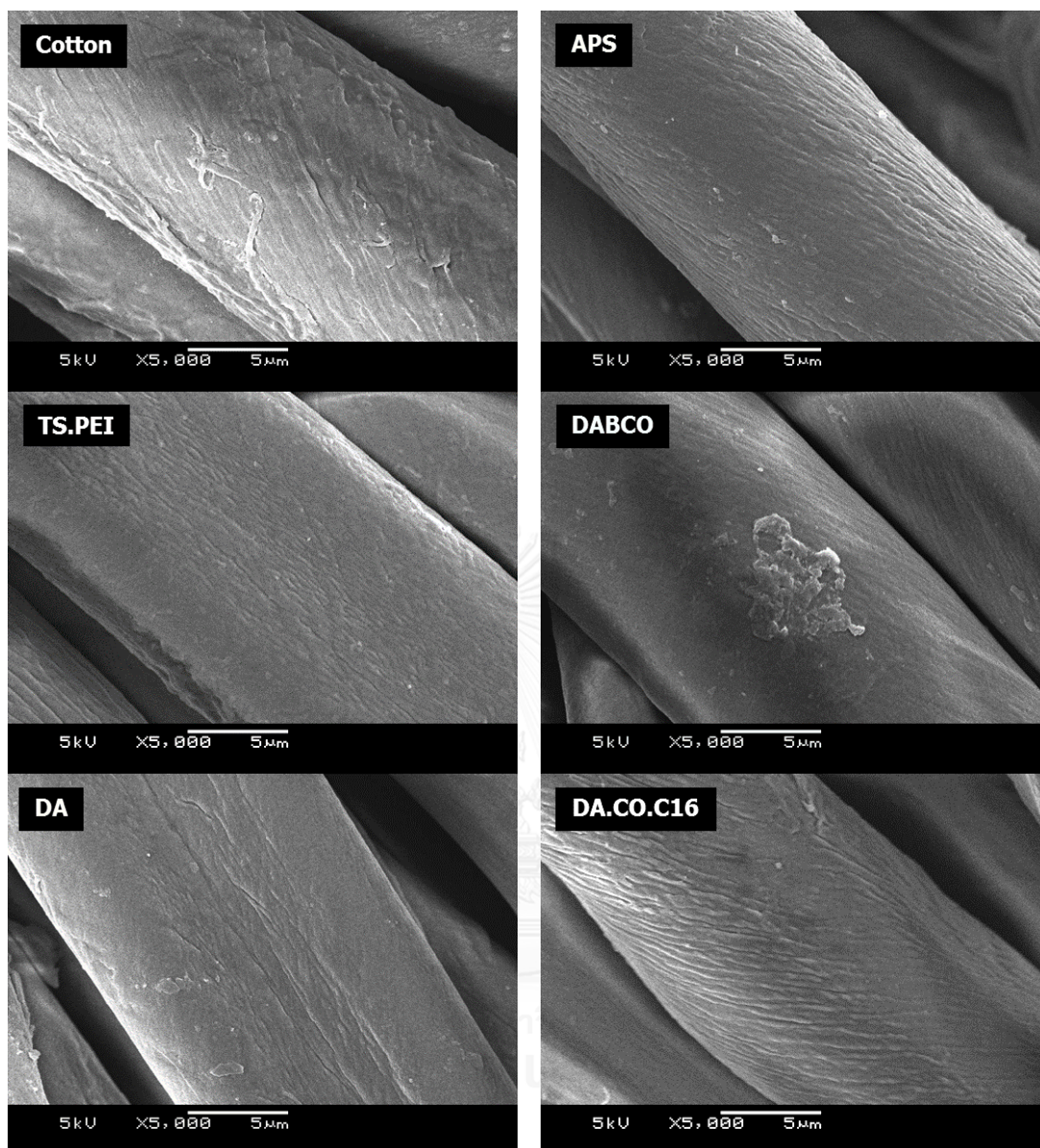


Figure 3.10 SEM images of unmodified and modified cotton with x5000 magnification.

### 3.3 Antibacterial activities

To evaluate antibacterial activities of all surfaces, antibacterial assays based on the Japanese Industrial Standard (JIS) L 1902 test were performed for at least three independent experiments using unmodified cotton as a negative control. Three species of bacteria including *Staphylococcus aureus* (ATCC 6538P), *Escherichia coli* (ATCC 8739) and *Pseudomonas aeruginosa* (ATCC 9027) were selected. All bacteria were cultured in Nutrient Broth (NB) media (pH 7.4±0.2) at 37 °C and the time period of bacterial contact on surfaces was 18 hours.

Antibacterial activities against *Staphylococcus aureus* are revealed in **Figure 3.11A**). Unmodified cotton showed high amount of bacterial growth around six log CFU. **APS** exhibited strong killing activities against this strain with essentially no colony observed. This strong inhibitory effect may be due to the highest primary amine loading amount among all surfaces, which in turn resulted in several available amino groups to be protonated to yield positive charges on the surface. These positive charges can then bind with lipoteichoic acid [19] and other anionic phospholipid contents including phosphatidylglycerol and phosphatidylserine on the membrane of Gram-positive bacteria via an electrostatic adhesive force [26]. The phospholipid contents may be pulled out of the bacterial membrane causing holes in the membrane. In addition, the fact that **APS** was synthesized on a support of polysiloxane may result in an increase in accessibility of the aminopropyl group to the membrane component of the bacterium, which is in contrast to some surfaces that active groups may stay close to the cellulose structure. The same argument can be applied to both Gram-negative bacteria (*Escherichia coli* (**Figure 3.11B**) and *Pseudomonas aeruginosa* (**Figure 3.11C**)), albeit with lesser degree as complete killing was not observed.

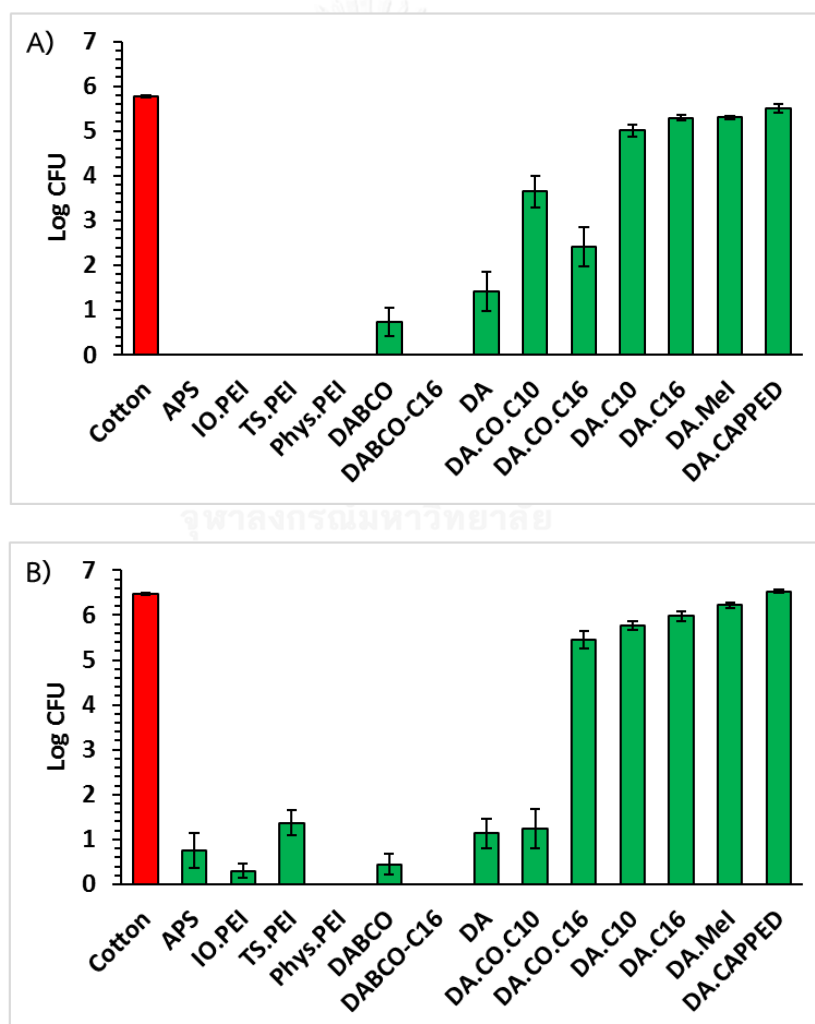
**PEIs** (**IO.PEI**, **TS.PEI**, **Phys.PEI**) showed high killing activities with no colony observed in *Staphylococcus aureus* since branched PEI is a polymer containing primary, secondary and tertiary amines which can be protonated. Similar to **APS**, the protonated amino groups can attract the negatively charged contents of cellular membrane and cause cell death. Interestingly, **Phys.PEI** seemed to be most active among all PEI surfaces for both Gram-negative bacteria with unknown reason.

Although **DABCO** did not show complete killing, the activity was still considered high with only one log CFU remained after exposure to the surface for all bacteria tested in this study. This is perhaps due to the monocationic structure. The permanent positive charge on quaternary amine can also interfere the structural integrities of bacterial membrane. Interestingly, no colony was observed on **DABCO-C16** with a polycationic structure and hydrophobic part. The cationic portions can interfere with membrane integrity and the lipophilic portion can attract to lipophilic moieties of lipid bilayer via hydrophobic interaction causing membrane destruction [26]. These same results occurred in Gram-negative bacteria, *Escherichia coli* (**Figure 3.11B**) and *Pseudomonas aeruginosa* (**Figure 3.11C**). The alkylation of **DABCO** can improve antibacterial efficiency in both Gram-positive and Gram-negative bacteria.

Notably, DA immobilized cotton was previously reported to show no antibacterial activities against methicillin-resistant *Staphylococcus aureus* (MRSA) by the Nakamura group [11]. Nevertheless, in this research, **DA** demonstrated high antibacterial activities against *Staphylococcus aureus* with four log CFU reduction. Since several experimental conditions are essentially identical, the difference in the exact strains used in each study may be the cause of this drastic difference in antibacterial activities. To gain further insight into this surprising activity, further modifications of **DA** were performed in order to probe structure-activity relationships. On the contrary to **DABCO**, the introduction of alkyl groups onto **DA** decreases antibacterial activities by reducing free amino groups for protonation. This was found to be true for **DA.C10**, **DA.C16**, **DA.Mel** and **DA.CAPPED** and for all species tested. However, the acylation of **DA** (**DA.CO.C10** and **DA.CO.C16**) showed some bacterial inhibitions related to the chain lengths. **DA.CO.C16** with a longer lipophilic chain showed higher antibacterial activities than **DA.CO.C10**.

In comparison with the Gram-positive *Staphylococcus aureus*, most surfaces showed similar activities to both *Escherichia coli* (**Figure 3.11B**) and *Pseudomonas aeruginosa* (**Figure 3.11C**). This is perhaps due to the fact that the positive charges of modified surfaces can attract to lipopolysaccharide on the outer membrane of Gram-negative bacteria via an electrostatic interaction [20]. However, Gram-negative bacterial membrane are more complex than Gram-positive bacteria. There are two layer of

membranes. An active portion must interact with both inner and outer membranes. Interestingly, apart from differences between Gram-positive and Gram-negative bacteria, some differences in activities of certain surfaces against each Gram-negative bacterium was also observed. **DA** and **DA.CO.C10** showed strong antibacterial activities in *Escherichia coli*, while **DA.CO.C16** was barely active. Conversely, **DA** and **DA.CO.C16** showed complete killing in *Pseudomonas aeruginosa*, while **DA.CO.C10** showed poor activities. These contrary results may be due to the difference of fatty acids substitution in lipopolysaccharide of the Gram-negative bacteria. *Pseudomonas aeruginosa* contains longer length of fatty acid chains than *Escherichia coli* [27-29].



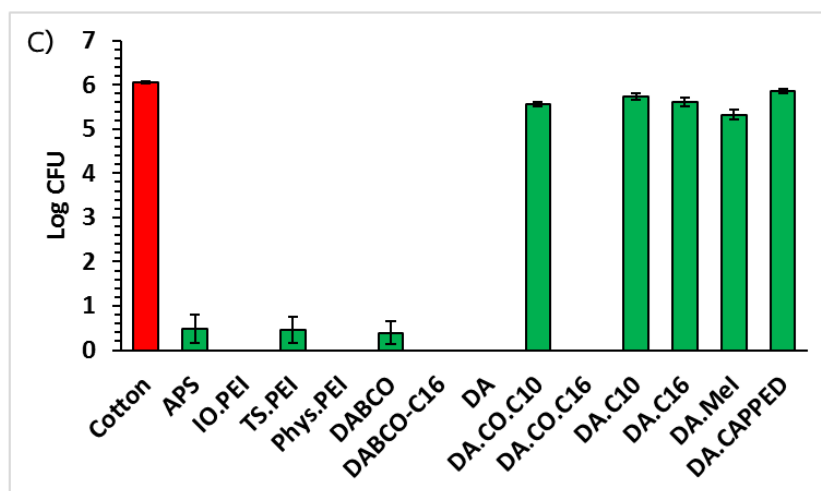


Figure 3.11 Log CFU of A) *Staphylococcus aureus* B) *Escherichia coli* C) *Pseudomonas aeruginosa* after 18-h incubation on various surfaces.

### 3.4 Inhibitory activities against foodborne pathogens

To gain further insight for possible food applications, inhibitory activities of modified cotton were tested against five species of foodborne pathogens; *Escherichia coli* (IAM 1264), *Leuconostoc carnosum* (JCM 9695), *Listeria monocytogenes* (CIP 103575), *Salmonella enterica* subsp. *enterica* (ATCC 13311) and *Acinetobacter baumannii* (JCM 6841). Culture conditions depend on each pathogen and the time period of bacterial contact on surfaces was 18 hours for all pathogens.

As pointed out in **Figure 3.12 A)** and **B)**, **APS** exhibited strong inhibitory activities in all species, especially complete killing was observed in both species of Gram-positive bacteria. Although **DA** did not show large amount of CFU reduction, the percentage of bacterial inhibitions were higher than 84% in *Escherichia coli*, *Salmonella enterica* subsp. *enterica* and *Leuconostoc carnosum*. Interestingly, the introduction of decanoic acid onto **DA** (**DA.CO.C10**) can improve inhibitory activities of surface **DA** with 97% bacterial inhibition in *Listeria monocytogenes*, whereas **DA** showed only 53% inhibition. Interestingly, **DA.C10** showed low inhibitory activities in all species, which corroborated well with the results from three strains studied in the previous section.

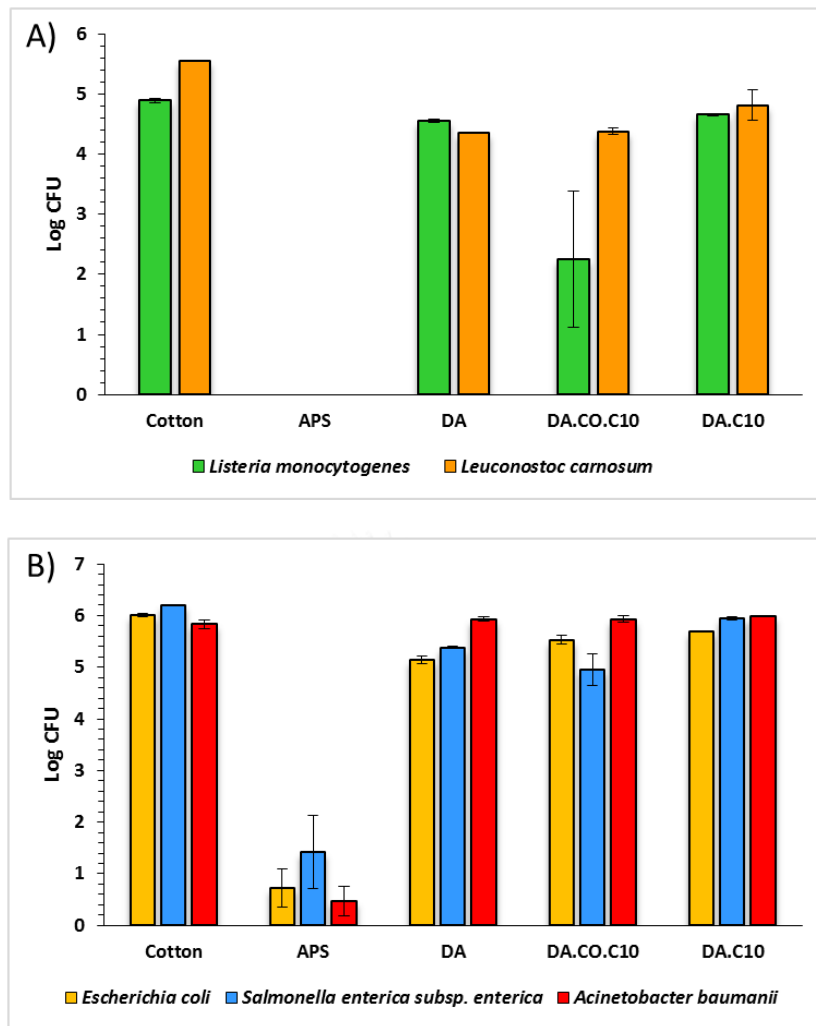


Figure 3.12 Log CFU of A) Gram-positive and B) Gram-negative foodborne pathogens after 18-h incubation on various surfaces.



### 3.5 Cytotoxicity

To ensure that fabricated surfaces can be applied for broader applications like in medical-related materials, cytotoxicity assays of modified cottons toward L-929 mouse connective tissue fibroblast were conducted. The cytotoxicity was measured by the standard MTT assay. In this regard, cotton was applied as a control sample with 100% cell growth. As shown in **Figure 3.13**, cell viability was estimated to be 113% for **DABCO** and around 80-85% for **DA** derivatives after 24 hours incubation. The results remained unchanged after 48 and 72 hours of incubation. These data indicated that **DABCO**, **DA** and **DA.CO.C16** are biocompatible with mammalian cell. In the case of **TS.PEI** and **Phys.PEI**, cell viability was nearly 20% after 24 hour-incubation and decreased to around 10% after 48 and 72 hours of incubation. The results demonstrate that PEIs modified surfaces did not exhibit sufficiently good biocompatibility. Nevertheless, **Phys.PEI** was easily fabricated and showed high antibacterial activities. Therefore, it may find some use in other applications with no direct contact with human cells.

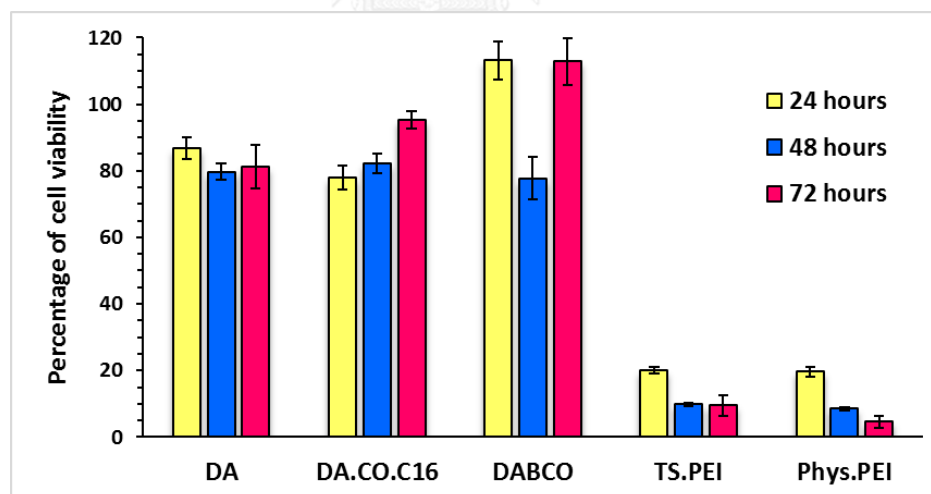


Figure 3.13 Cell viability on modified surfaces using L-929 cell line

## CHAPTER IV

### CONCLUSIONS

A series of amino-containing molecules, namely 3-aminopropyltrimethoxy silane (**APS**), polyethyleneimine (**PEI**), 1,4-diazabicyclo[2.2.2]octane (**DABCO**), 4,7,10-trioxa-1,13-tridecanediamine (**DA**) immobilized on cotton surfaces were successfully fabricated using various chemical reactions. Additionally, **DA** was further modified with various capping reagents to investigate some structure-activity relationship. Antibacterial activities of all surfaces were evaluated in both Gram-positive (*Staphylococcus aureus* (ATCC 6538P) and Gram-negative bacteria (*Escherichia coli* (ATCC 8739) and *Pseudomonas aeruginosa* (ATCC 9027)). **DABCO-C16** with polycationic structure and **Phys.PEI** with its abilities to be protonated showed complete killing in all species. **APS** and **DA** also have the protonating abilities. These surfaces showed non-complete killing, but were still considered highly active with around five log CFU reduction. Their bacterial growth inhibition on Gram-positive bacteria were higher than that of Gram-negative bacteria due to the difference of membrane components. Cytotoxicity assays of modified cottons toward L-929 mouse connective tissue fibroblast were evaluated and confirmed the biocompatibilities of **DABCO** and **DA** and its derivative with mammalian cells.

Due to the broad spectrum of antibacterial activities of fabricated surfaces, assays related to food applications were also performed. In this regard, five species of foodborne pathogens (*Escherichia coli* (IAM 1264), *Salmonella enterica* subsp. *enterica* (ATCC 13311), *Acinetobacter baumannii* (JCM 6841), *Listeria monocytogenes* (CIP 103575) and *Leuconostoc carnosum* (JCM 9695)) were used to evaluate inhibitory activities of modified cotton. **APS** showed high bacterial growth inhibitions in all species. Interestingly, the modification of **DA** with decanoic acid (**DA.CO.C10**) can increase inhibitory activities in *Salmonella enterica* subsp. *enterica* and *Listeria monocytogenes*.

## REFERENCES

- [1] Siedenbiedel, F. and Tiller, J.C. Antimicrobial Polymers in Solution and on Surfaces: Overview and Functional Principles. Polymers 4(1) (2012): 46.
- [2] Selner, M.Y., Winnie; Watson, Kathryn; Kim, Steven. Food Poisoning Healthline [Online]. 2015. Available from: <http://www.healthline.com/health/food-poisoning#Overview1> [27 April 2016]
- [3] Green, D.W. The bacterial cell wall as a source of antibacterial targets. Expert Opinion on Therapeutic Targets 6(1) (2002): 1-20.
- [4] Yu, Q., Wu, Z., and Chen, H. Dual-function antibacterial surfaces for biomedical applications. Acta Biomaterialia 16 (2015): 1-13.
- [5] Xu, L.-C. and Siedlecki, C.A. Protein adsorption, platelet adhesion, and bacterial adhesion to polyethylene-glycol-textured polyurethane biomaterial surfaces. Journal of Biomedical Materials Research Part B: Applied Biomaterials (2015): n/a-n/a.
- [6] Knetsch, M.L.W. and Koole, L.H. New Strategies in the Development of Antimicrobial Coatings: The Example of Increasing Usage of Silver and Silver Nanoparticles. Polymers 3(1) (2011): 340.
- [7] Mayr, M., Kim, M.J., Wanner, D., Helmut, H., Schroeder, J., and Mihatsch, M.J. Argyria and Decreased Kidney Function: Are Silver Compounds Toxic to the Kidney? American Journal of Kidney Diseases 53(5) (2009): 890-894.
- [8] Abel, T., Cohen, J.I., Engel, R., Filshtinskaya, M., Melkonian, A., and Melkonian, K. Preparation and investigation of antibacterial carbohydrate-based surfaces. Carbohydrate Research 337(24) (2002): 2495-2499.
- [9] Chaker, A. and Boufi, S. Cationic nanofibrillar cellulose with high antibacterial properties. Carbohydrate Polymers 131 (2015): 224-232.
- [10] Fernandes, S.C.M., et al. Bioinspired Antimicrobial and Biocompatible Bacterial Cellulose Membranes Obtained by Surface Functionalization with Aminoalkyl Groups. ACS Applied Materials & Interfaces 5(8) (2013): 3290-3297.

- [11] Nakamura, M., Iwasaki, T., Tokino, S., Asaoka, A., Yamakawa, M., and Ishibashi, J. Development of a Bioactive Fiber with Immobilized Synthetic Peptides Designed from the Active Site of a Beetle Defensin. Biomacromolecules 12(5) (2011): 1540-1545.
- [12] Shalev, T., Gopin, A., Bauer, M., Stark, R.W., and Rahimpour, S. Non-leaching antimicrobial surfaces through polydopamine bio-inspired coating of quaternary ammonium salts or an ultrashort antimicrobial lipopeptide. Journal of Materials Chemistry 22(5) (2012): 2026-2032.
- [13] Valotteau, C., et al. Biocidal Properties of a Glycosylated Surface: Sophorolipids on Au(111). ACS Applied Materials & Interfaces 7(32) (2015): 18086-18095.
- [14] Dacarro, G., Cucca, L., Grisoli, P., Pallavicini, P., Patrini, M., and Taglietti, A. Monolayers of polyethylenimine on flat glass: a versatile platform for cations coordination and nanoparticles grafting in the preparation of antibacterial surfaces. Dalton Transactions 41(8) (2012): 2456-2463.
- [15] Lin, J., Qiu, S., Lewis, K., and Klibanov, A.M. Mechanism of bactericidal and fungicidal activities of textiles covalently modified with alkylated polyethylenimine. Biotechnology and Bioengineering 83(2) (2003): 168-172.
- [16] Gultekinoglu, M., et al. Designing of dynamic polyethyleneimine (PEI) brushes on polyurethane (PU) ureteral stents to prevent infections. Acta Biomaterialia 21 (2015): 44-54.
- [17] Klemm, D., Schmauder, H.-P., and Heinze, T. Cellulose. in Biopolymers Online: Wiley-VCH Verlag GmbH & Co. KGaA, 2005.
- [18] Siqueira, G., Bras, J., and Dufresne, A. Cellulosic Bionanocomposites: A Review of Preparation, Properties and Applications. Polymers 2(4) (2010): 728.
- [19] Scott, M.G., Gold, M.R., and Hancock, R.E.W. Interaction of Cationic Peptides with Lipoteichoic Acid and Gram-Positive Bacteria. Infection and Immunity 67(12) (1999): 6445-6453.
- [20] Prokhorenko, I.R., Zubova, S.V., Ivanov, A.Y., and Grachev, S.V. Interaction of Gram-negative bacteria with cationic proteins: Dependence on the surface characteristics of the bacterial cell. International Journal of General Medicine 2 (2009): 33-38.

- [21] Thomas, M., et al. Polycations. 17. Synthesis and properties of polycationic derivatives of carbohydrates. Carbohydrate Research 344(13) (2009): 1620-1627.
- [22] Hsu, B.B. and Klibanov, A.M. Light-Activated Covalent Coating of Cotton with Bactericidal Hydrophobic Polycations. Biomacromolecules 12(1) (2011): 6-9.
- [23] Mazzei, P., Fusco, L., and Piccolo, A. Acetone-induced polymerisation of 3-aminopropyltrimethoxysilane (APTMS) as revealed by NMR spectroscopy. Magnetic Resonance in Chemistry 52(7) (2014): 383-388.
- [24] Noel, S., Liberelle, B., Robitaille, L., and De Crescenzo, G. Quantification of Primary Amine Groups Available for Subsequent Biofunctionalization of Polymer Surfaces. Bioconjugate Chemistry 22(8) (2011): 1690-1699.
- [25] Grumezescu, V., et al. Fabrication and characterization of functionalized surfaces with 3-amino propyltrimethoxysilane films for anti-infective therapy applications. Applied Surface Science 336 (2015): 401-406.
- [26] Yatvin, J., Gao, J., and Locklin, J. Durable defense: robust and varied attachment of non-leaching poly"-onium" bactericidal coatings to reactive and inert surfaces. Chemical Communications 50(67) (2014): 9433-9442.
- [27] Emiola, A., George, J., and Andrews, S.S. A Complete Pathway Model for Lipid A Biosynthesis in *Escherichia coli*. PLoS ONE 10(4) (2015): e0121216.
- [28] Pier, G.B. Pseudomonas aeruginosa lipopolysaccharide: a major virulence factor, initiator of inflammation and target for effective immunity. Int J Med Microbiol 297(5) (2007): 277-95.
- [29] Ernst, R.K., et al. Unique Lipid A Modifications in Pseudomonas aeruginosa Isolated from the Airways of Patients with Cystic Fibrosis. The Journal of infectious diseases 196(7) (2007): 1088-1092.



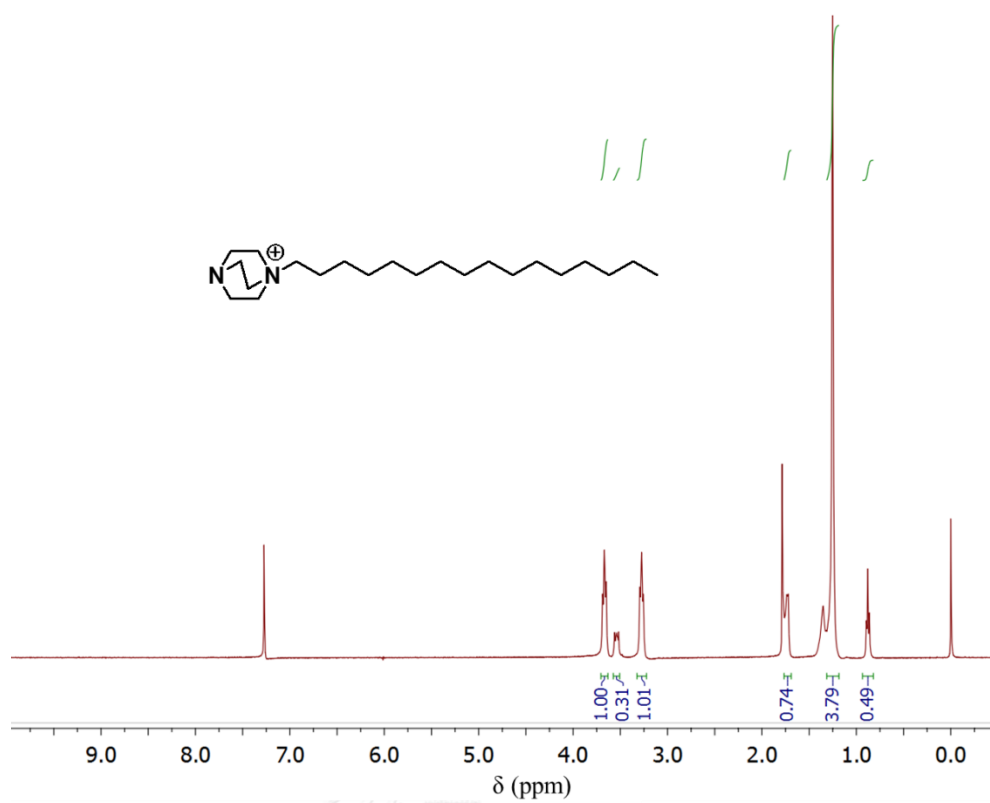


Figure A1  $^1\text{H}$  NMR spectrum of the precursor molecule for DABCO.C16 fabrication.

## VITA

Ms. Monrawat Rauytanapanit was born on 13th May, 1991 in Ratchaburi, Thailand. She graduated Bachelor's degree in Chemistry with second class honors from Kasetsart University in 2013. She has got a scholarship from the Development and Promotion of Science and Technology Talents Project (DPST). She had an opportunity to do the research in Tokyo University of Marine Science and Technology, Japan in 2016. She has been a graduate student in the Department of Chemistry, Faculty of Science, Chulalongkorn University and worked under the supervision of Dr.Thanit Praneenararat since 2013.

